

The role of magmatic reaction, diffusion and annealing in the evolution of coronitic microstructure in troctolitic gabbro from Risør, Norway

RAYMOND JOESTEN

Department of Geology and Geophysics, The University of Connecticut, Storrs, CT 06268 USA

ABSTRACT. Coronas of symplectic pargasite [$X_{Mg} = 68$, $X_{Ca} = 69$, $X_{Si} = 68$] + spinel [$SP_{4.5}$] and orthopyroxene [EN_{70}] separate cumulus plagioclase [$AN_{6.4}$] and olivine [$FO_{6.4}$] in troctolitic gabbro from Risør, Norway. Coronas with a primary microstructure characterized by low-angle grain boundaries have the mineral assemblage layer sequence,

PLAGIOCLASE : PARGASITE + SPINEL : ORTHOPYROXENE +
SPINEL : ORTHOPYROXENE : OLIVINE,

whereas those with an annealed microstructure have the layer sequence,

PLAGIOCLASE : PARGASITE + SPINEL :
PARGASITE : ORTHOPYROXENE : OLIVINE.

Primary symplectite consists of fan-shaped grains of pargasite that open toward plagioclase and are ribbed by rods of spinel. On annealing to a single grain, low-angle grain boundaries disappear and spinel rods rotate into parallel positions. Primary orthopyroxene, initially radial to layer contacts, anneals to a single grain, rimming olivine. Irregular discontinuous layers and plumes of symplectic orthopyroxene + spinel disappear on annealing and a monomineralic layer of pargasite forms between orthopyroxene and the amphibole symplectite.

The identity of composition of intercumulus pargasite and orthopyroxene with the same phases in primary coronas, the occurrence of primary and annealed coronas rimming cumulus ilmenite and the occurrence of radial orthopyroxene separating grains of cumulus olivine and separating cumulus olivine and plagioclase argue for the origin of primary coronas by fractional crystallization of spinel-saturated troctolitic magma at a pressure greater than 5 kbar.

Irreversible thermodynamic calculations show that the mineral assemblage layer sequence of the primary coronas is diffusively unstable and that this instability provides the driving force for their spontaneous transformation to the stable mineral assemblage layer sequence of the annealed coronas.

KEYWORDS: magmatism, diffusion, annealing, coronas, gabbro, Risør, Norway.

These zones of new-formed minerals have evidently originated through an interaction between plagioclase and olivine. . . . That this is so appears from the fact that the zones always occur where olivine and feldspar are adjacent, but are lacking between olivine and augite.

A. E. TÖRNEBOHM (1877)

It is the consensus that olivine coronas made up of concentric layers of orthopyroxene and either amphibole + spinel, clinopyroxene + spinel or clinopyroxene + garnet, form by metamorphic reaction and mass transfer between olivine and enveloping plagioclase, an idea that traces its roots to Törnebohm (1877), Sederholm (1916), and Brögger (1934). The consistent textural relation cited by Törnebohm has been observed repeatedly in olivine gabbros from amphibolite-facies (Murthy, 1958; Reynolds and Frederickson, 1962; Mason, 1967; Grieve and Gittins, 1975; van Lamoen, 1979; and Mongkoltip and Ashworth, 1983) and granulite-facies (Griffin and Heier, 1973; Whitney and McLelland, 1973; McLelland and Whitney, 1977, 1980a and b) metamorphic terranes the world over. Current questions centre on the timing of corona growth relative to the emplacement and cooling of the gabbro body and to subsequent metamorphism (Griffin and Heier, 1973; Whitney and McLelland, 1973; and Mongkoltip and Ashworth, 1983) and on the calculation of mass transfer between olivine and plagioclase (Whitney and McLelland, 1973; Grieve and Gittins, 1975; McLelland and Whitney, 1977; and Nishiyama, 1983) or between olivine, plagioclase, and intergranular fluid (van Lamoen, 1979, and Mongkoltip and Ashworth, 1983).

Discordant bodies of troctolite and olivine gabbro of Precambrian age on the Risør peninsula on the south-eastern coast of Norway each have a

coronitic core that passes outward into an amphibolitic margin. The petrology of the gabbroic suite is described by Starmer (1969), who suggested a post-consolidation metamorphic origin for the coronas. Radiometric ages of gabbro crystallization and metamorphism have not been determined, however.

Primary intercumulus and coronitic microstructures are unusually well developed and well preserved in troctolitic gabbro from Risør, Norway. On the basis of textural and compositional relations described in this paper, it is argued that primary as-grown corona microstructures in the Risør troctolite are of magmatic origin and that they record the effects of a subsequent annealing process.

The sample of troctolitic gabbro from Risør described in this paper consists of tabular laths of plagioclase, elongated parallel to (010), with triangular interstices between laths occupied by ferromagnesian and oxide minerals. Cumulus olivine, initially in contact with cumulus plagioclase or melt shows three rimming sequences. That consisting of successive rims of orthopyroxene, clinopyroxene and pargasitic amphibole is clearly derived by crystallization of intercumulus liquid. Rimming sequences with a pargasite-spinel symplectite separating orthopyroxene and plagioclase possess the typical corona microstructure. Microstructures of the orthopyroxene layer and of the pargasite + spinel symplectite in coronas record both primary growth and subsequent annealing.

The original purpose of this study was the measurement of mass transfer between olivine and plagioclase as recorded by the coronas for comparison with the mass transfer predicted by a model for diffusion-controlled corona growth using the methods of nonequilibrium thermodynamics (Fisher, 1973, 1977; Joesten, 1977; Nishiyama, 1983). These calculations show, however, that the mineral assemblage layer sequence of primary coronas is diffusionally unstable along the chemical potential gradients established across the structure by local equilibrium and buffering at layer contacts. Thus, to the extent that behaviour of the model system can be used to predict behaviour of the real system, primary coronas cannot have been formed by diffusional exchange of material between olivine and plagioclase and, irrespective of how they were formed, they should have spontaneously transformed to a stable sequence of mineral assemblage layers. Similar modelling of annealed coronas demonstrates the diffusional stability of their mineral assemblage layer sequence and tightly constrains relative values of the Onsager diffusion constants for Mg, Al, and Si.

The argument that primary as-grown corona

microstructures are of magmatic origin and that they have subsequently annealed is based essentially on textural evidence. It is supported by the identity of composition of individual phases in each of the three textural associations and by the bulk mineralogical and chemical compositions of corona structures. Irreversible thermodynamic calculations merely show that primary corona structures in the model system are diffusionally unstable and that this instability may provide the driving force for conversion to the diffusionally stable mineral assemblage layer sequence of annealed coronas.

The textural and compositional observations that support the argument for magmatic corona growth and subsequent annealing are detailed below. Most of the textural and compositional features that are inconsistent with diffusion-controlled growth of coronas by exchange between olivine and plagioclase have been described before (Brögger, 1934; van Lamoen, 1979; and Mongkoltip and Ashworth, 1983) and essentially all evidence previously cited in support of a metamorphic origin for coronas is consistent with the model developed here. However, the primary support for a metamorphic origin for coronas rests on a single, unanswerable argument, namely that because coronas in gabbro from high-grade metamorphic terranes everywhere separate olivine and plagioclase, they necessarily form by reaction and exchange between solid olivine and plagioclase. This paper is intentionally written in an interpretative, advocative style, to call attention to those textural and compositional features consistent with a magmatic origin for the coronas and which make a metamorphic origin untenable.

The sample described in this study is number 3085 from the Harker Collection of Cambridge University, collected by W. C. Brögger and provided through the kindness of Stuart Agrell and Graham Chinner. It is the sample illustrated in by Harker in *The Natural History of Igneous Rocks* (Harker, 1909, fig. 88A), and later by Chinner in *Petrology for Students* (Nockolds *et al.*, 1978, fig. 33-7A).

MICROSTRUCTURE OF THE MAGMATIC ASSEMBLAGE

Although it will be demonstrated below that growth of the primary corona microstructure is a magmatic phenomenon, it is useful to designate those minerals whose rimming relations are clearly the result of crystallization from intercumulus liquid as the magmatic assemblage. Textural relations of the magmatic mineral assemblage are illustrated in the micrograph of fig. 1 (left side,

TABLE I
ELECTRON MICROPROBE ANALYSES - MAGMATIC MINERAL ASSEMBLAGE

	WEIGHT PERCENT OXIDE				
	OL	OPX	CPX	AMP	PLAG
SiO ₂	36.71	55.12	51.26	42.03	53.48
TiO ₂	-	-	0.84	2.36	-
Al ₂ O ₃	-	1.47	4.97	16.04	31.23
Cr ₂ O ₃	-	-	0.34	0.19	-
FeO	30.81	18.57	6.54	9.78	0.17
MnO	0.30	0.31	0.09	-	-
MgO	31.74	26.25	14.35	12.85	-
CaO	0.12	0.28	20.66	11.55	13.17
Na ₂ O	-	-	0.87	2.72	4.09
K ₂ O	-	-	-	0.72	-
ΣOXIDES	99.69	102.01	99.93	98.23	102.14
	MINERAL FORMULA				
Si (4+)	1.000	1.968	1.888	6.080	2.372
Ti (4+)	-	-	0.023	0.257	-
Al (3+)	-	0.062	0.216	0.735	1.633
Cr (3+)	-	-	0.010	0.022	-
Fe (2+)	0.702	0.554	0.202	1.184	0.006
Mn (2+)	0.007	0.009	0.003	-	-
Mg (2+)	1.288	1.396	0.788	2.770	-
Ca (2+)	0.004	0.011	0.815	1.790	0.626
Na (1+)	-	-	0.063	0.762	0.351
K (1+)	-	-	-	0.133	-
ΣCATIONS	3.000	4.001	4.007	15.732	4.992
ΣOXYGEN	4	6	6	23	8
Mg/Mg+Fe	0.645	0.716	0.796	0.700	-
Ca/Ca+Na	-	-	0.928	0.701	0.640
Al/(Al+Si)	-	0.031	0.103	0.310	0.408

bottom and far right) and representative electron probe analyses of minerals in this field of view are given in Table I.

Laths of plagioclase (AN₆₄₋₆₅), equant grains of olivine (FO₆₁₋₆₄) and tabular plates of ilmenite occur as cumulus phases. Olivine is rimmed by orthopyroxene (EN₇₀₋₇₂). Where the orthopyroxene is in contact with clinopyroxene, the rim is about 24 μm thick and consists of a single, optically continuous crystal. The contact with clinopyroxene tends to be ragged, but is sharp and planar where an amphibole-spinel symplectite is present (fig. 1, centre-left, fig. 2). Where olivine appears to have been in contact with plagioclase (fig. 1, centre-right), the orthopyroxene rim ranges from 72 to 105 μm in thickness and consists of radially arranged grains with low-angle grain boundaries, oriented perpendicular to the layer contact with olivine. The radial microstructure and those of the associated symplectites are described in the section on primary coronas.

Single crystals of intercumulus clinopyroxene, with normative composition WO₄₀EN₄₂FS₁₁JD₀₃

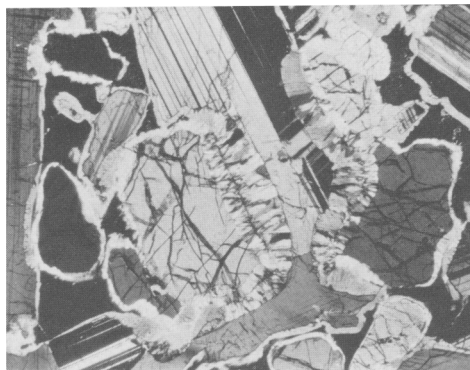


Fig. 1. Cumulus olivine crystals rimmed by intercumulus magmatic assemblage and primary corona assemblage. Two small olivines (left and bottom centre) rimmed by magmatic assemblage consisting of optically continuous rim of orthopyroxene (illuminated), enveloped by space-filling single crystal of intercumulus clinopyroxene (in extinction) with thin optically continuous rim of pargasite (illuminated). Large olivine (centre) rimmed on right side by primary corona assemblage along contact with plagioclase. Two olivine grains (right centre) rimmed on their left hand side by primary corona assemblage (lower) and by annealed corona assemblage (upper). Width of field, 3 mm, crossed polars.

MgTS₀₁TiCaTS₀₃, fill triangular interstices between plagioclase laths (fig. 1, centre-left, top and bottom). Individual, optically continuous crystals may extend over 10 mm. Rods of rutile crowd cores of clinopyroxene, but the rims are inclusion-free.

Clinopyroxene is separated from plagioclase by an optically continuous rim of pale-brown pargasitic amphibole, 12-18 μm in thickness. The clinopyroxene/amphibole and amphibole/plagioclase contacts are mutually parallel and parallel to (010) of the plagioclase.

Where the rim of clinopyroxene separating olivine and orthopyroxene from plagioclase is thin, the amphibole rim thickens slightly and consists of a symplectitic intergrowth with spinel in its outer part (fig. 2, fig. 1, centre-left). The volume fraction spinel in the symplectite is 0.098 ± 0.025. Where the magmatic amphibole-spinel symplectite is present, the clinopyroxene layer may be discontinuous, leaving amphibole locally in contact with orthopyroxene.

Where intercumulus clinopyroxene is absent, a large single crystal of amphibole may partially or wholly envelop a grain of cumulus olivine and fill the intercumulus space between olivine and laths of plagioclase. Amphibole in this association is separated from olivine by a rim of orthopyroxene that commonly possesses the radial microstructure

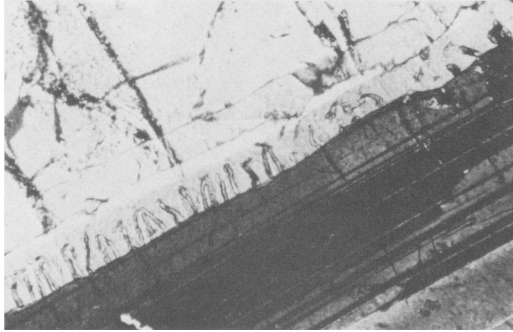


FIG. 2. Magmatic amphibole-spinel symplectite. Cumulus olivine, upper left, separated from plagioclase, lower right, by series of optically continuous rims of orthopyroxene, clinopyroxene, amphibole, and amphibole-spinel symplectite. Clinopyroxene rim pinches out at top right. Width of field, 0.54 mm, crossed polars.

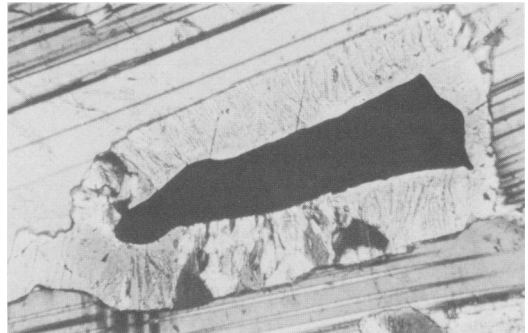


FIG. 3. Plate of cumulus ilmenite separated from plagioclase by magmatic amphibole (lower left and right centre), primary amphibole-spinel symplectite (bottom centre), and annealed amphibole-spinel symplectite and monomineralic amphibole layer (top and bottom right). Width of field, 0.54 mm, crossed polars.

described below. Locally, thin spears of orthopyroxene emanating from the orthopyroxene rim are epitaxially intergrown with amphibole. Ilmenite invariably occurs in this association and the intercumulus amphibole has the brown absorption colour characteristic of Ti-enriched amphibole. Large grains of intercumulus amphibole locally contain symplectitically intergrown spinel in a rim 100 μm in thickness on its outer margin (fig. 6, centre-right).

Ilmenite plates are everywhere separated from plagioclase by a rim of amphibole or amphibole-spinel symplectite (fig. 3, Table IV). Neither ortho- nor clinopyroxene occur in association with ilmenite. Spinel occurs both as blocky grains intergrown with ilmenite and in the symplectite. Amphibole associated with ilmenite is deeper brown in colour than that associated with pyroxene and is very slightly enriched in Ti and depleted in Si. Absorption colour and composition of amphibole in contact with spinel are identical to those of amphibole in contact with ilmenite.

The contact between ilmenite and symplectite may be planar or convex toward ilmenite. Where significant curvature occurs, ilmenite grains thin toward their ends and terminate in a cusp, indicative of significant loss by resorption or reaction.

Amphibole has three distinct textural habits where it rims ilmenite, two of which involve symplectitic intergrowths with spinel. Amphibole-spinel symplectite, characterized by fan-shaped amphibole grains with subparallel grain boundaries (fig. 3, bottom centre), is interpreted below to be a primary, as-grown microstructure. Many ilmenite grains are almost completely rimmed by a single,

optically continuous amphibole grain. This grain may be free of spinel inclusions (fig. 3, lower left and upper right), but along much of its length it consists of a symplectitic intergrowth with spinel in its outer part with a thin rim of inclusion-free amphibole in contact with ilmenite (fig. 3, top and lower right). The microstructure of the amphibole-spinel symplectite is unchanged where it passes along its length from contact with ilmenite to contact with spinel.

MICROSTRUCTURE OF OLIVINE CORONAS

Throughout the sample, olivine is separated from plagioclase by a corona having a layer of orthopyroxene in contact with olivine and an amphibole-spinel symplectite in contact with plagioclase. Olivine coronas exhibit two microstructural types, interpreted as primary and annealed, each with a characteristic mineral assemblage layer sequence. Both the primary corona (fig. 4, top) and annealed corona (fig. 4, bottom) microstructures may occur on a single grain of olivine and each may pass, along its length, into the magmatic rimming sequence.

Primary coronas are characterized by radially arranged crystals of orthopyroxene and amphibole with low-angle grain boundaries. On annealed coronas, orthopyroxene and the amphibole of the symplectite each occur as single, optically continuous crystals, rimming olivine. It is because low-angle grain boundaries in metals and ceramics can be eliminated by heat treatment, that coronas with low-angle grain boundaries are identified as primary whereas those with single crystal

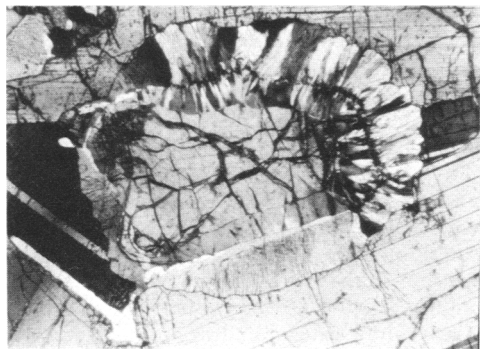


FIG. 4. Cumulus olivine rimmed by primary corona assemblage (top and right), annealed corona assemblage (bottom), and magmatic assemblage (left). Speck of clinopyroxene between cumulus plagioclase grains (lower left) is optically continuous with clinopyroxene lenses at lower end of corona. Width of field, 2 mm, crossed polars.

orthopyroxene and amphibole are identified as their annealed equivalents.

Primary coronas have an irregular, discontinuous layer of orthopyroxene-spinel symplectite separating the orthopyroxene layer and the amphibole-spinel symplectite. The mineral assemblage layer sequence of primary coronas is thus

OLIVINE : ORTHOPYROXENE : ORTHOPYROXENE +
SPINEL : AMPHIBOLE + SPINEL : PLAGIOCLASE.

Annealed coronas have a layer of inclusion-free amphibole between the orthopyroxene layer and the symplectite. Monomineralic amphibole is optically continuous with the amphibole of the symplectite. The mineral assemblage layer sequence of annealed coronas is thus

OLIVINE : ORTHOPYROXENE : AMPHIBOLE :
AMPHIBOLE + SPINEL : PLAGIOCLASE.

Details of corona microstructures are enhanced by etching of a polished thin section with HF fumes and imaging the surface with the Normarski interference method (figs. 5B, 7, and 9B). Layer widths were measured on polished and etched thin sections using a micrometer eyepiece and reflected light and were measured on photomicrographs. Modal analyses of symplectites were made by repetitive counting of intercepts on a 100 line micrometer eyepiece on polished and etched thin sections and by similar measurement on photomicrographs. Bulk chemical composition of symplectites was computed using the mode and electron probe analyses of orthopyroxene or amphibole, and spinel.

MICROSTRUCTURE OF PRIMARY CORONAS

The radial arrangement of grains around olivine in the orthopyroxene and amphibole-spinel symplectite layers is the characterizing feature of primary coronas. The microstructure of the primary corona shown in fig. 1 (right-hand side of olivine in centre of field) is illustrated in the micrographs of fig. 5A and B and representative electron probe analyses of minerals in this corona are listed in Table II.

Orthopyroxene layer

The orthopyroxene layer in primary coronas consists of radially arranged grains with low-angle grain boundaries, oriented at a high angle to the layer contact with olivine (fig. 5A). Individual grains are triangular in section, with the short side on or close to one of the layer contacts. The number of

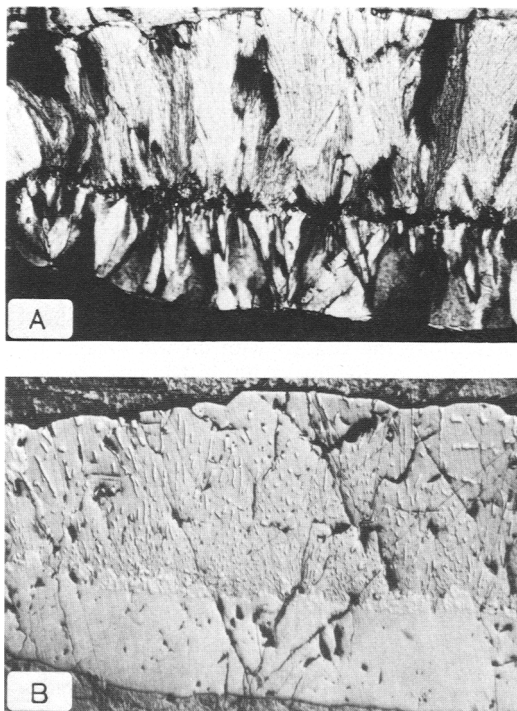


FIG. 5. Primary corona microstructure of olivine illustrated in fig. 1 (right). Olivine (bottom) separated from plagioclase (top) by layer of radial orthopyroxene, irregular layer of orthopyroxene-spinel symplectite, and fanning aggregate of amphibole-spinel symplectite. Electron probe analyses in Table II are from grains in this field of view. Width of field, 0.54 mm. A. Crossed polars. B. Reflected light, Normarski interference image of etched surface.

TABLE II
ELECTRON MICROPROBE ANALYSES - PRIMARY CORONA ASSEMBLAGE

	WEIGHT PERCENT OXIDE				
	OL	OPX	AMP	SP	PLAG
SiO ₂	36.74	54.31	42.76	-	53.11
TiO ₂	-	-	0.03	-	-
Al ₂ O ₃	-	1.68	17.58	63.93	30.97
Cr ₂ O ₃	-	-	-	-	-
FeO	34.18	19.27	9.76	24.54	0.20
MnO	0.29	0.32	-	-	-
MgO	28.84	24.79	13.80	11.48	-
CaO	-	0.28	11.80	-	13.03
Na ₂ O	-	-	2.71	-	4.01
K ₂ O	-	-	0.85	-	0.02
ΣOXIDES	100.06	100.66	99.28	100.00	101.35
	MINERAL FORMULA				
Si (4+)	1.012	1.972	6.100	-	2.373
Ti (4+)	-	-	0.035	-	-
Al (3+)	-	0.072	2.957	2.000	1.632
Cr (3+)	-	-	-	-	-
Fe (2+)	0.787	0.585	1.165	0.546	0.008
Mn (2+)	0.007	0.010	-	-	-
Mg (2+)	1.183	1.342	2.935	0.459	-
Ca (2+)	-	0.011	1.805	-	0.624
Na (1+)	-	-	0.750	-	0.347
K (1+)	-	-	0.155	-	0.001
ΣCATIONS	2.988	3.992	15.870	3.000	4.985
ΣOXYGEN	4	6	23	4	8
Mg/Mg+Fe	0.600	0.696	0.716	0.459	-
Ca/Ca+Na	-	-	0.706	-	0.643
Al/Al+Si	-	0.035	0.326	1.0	0.407

crystals per unit length of contact is greater along the contact with orthopyroxene-spinel symplectite than along the contact with olivine. Grains that extend across the full width of the layer are those with an apex at the outer contact with symplectite and their base on the inner contact with olivine. Grains with their base on the outer contact tend to pinch out part of the way across the layer.

These observations are consistent with nucleation of orthopyroxene at the outer edge of the layer and growth inward at the expense of olivine by columnar impingement. Columnar impingement microstructure results when grains nucleate along a surface and grow into the reactant material. In the competition for space, those grains oriented with their fast growth direction approximately perpendicular to the surface are favoured and growth of these grains crowds out other grains. Optimally oriented grains grow across the full width of the layer while less favourably orientated grains are pinched out.

The inner contact of the orthopyroxene layer with olivine is gently undulating and tends to be convex toward the olivine core. Where the radius of curvature is large, the contact is smoothly curved

around corners on the olivine grain (figs. 1 and 4), but where it is small, the contact has a cusp (fig. 6, centre-right). In the extreme, the cusp may be sufficiently deep so that the orthopyroxene layers from both sides of the corona are in contact along their original contact with olivine (fig. 6).

Olivine grains with cusped contacts are those that appear smallest in section and on which the orthopyroxene and symplectite layers have the greatest apparent thickness. These features are consistent both with these coronas having been sectioned far off-centre and with the olivine having suffered more extensive dissolution or reaction than its counterparts that occur as larger grains with smoothly curving contacts.

The apparent thickness of the orthopyroxene layer in thin section ranges from 72 to 105 μm on different coronas. However, layer thickness typically varies by $\pm 5 \mu\text{m}$ along planar segments of layers on a given corona. The outer contact with the orthopyroxene-spinel symplectite is planar.

Columnar impingement orthopyroxene, characteristic of primary coronas, locally occurs as a rim separating cumulus olivine and intercumulus amphibole and may occur as slender spears epitaxially intergrown with the amphibole. There are a number of cases in which a single columnar impingement layer of orthopyroxene may separate two grains of cumulus olivine. These observations



FIG. 6. Primary coronas on cumulus olivine. Extensive dissolution of olivine core brings orthopyroxene layers into contact along original OPX:OL contact (left centre). Primary corona assemblage on right margin of olivine at right now in contact with amphibole-spinel symplectite on magmatic amphibole. Amphibole in annealed symplectite on olivine at right is in optical continuity with adjacent magmatic amphibole. These observations suggest that primary corona microstructure developed before olivine came into contact with magmatic amphibole and that annealing occurred afterward. Width of field, 2 mm, crossed polars.



FIG. 7. Primary corona microstructure. Orthopyroxene (top) separated from plagioclase (bottom) by amphibole-spinel symplectite. Plumes of orthopyroxene-spinel symplectite stand out in relief against amphibole-spinel symplectite. Width of field, 0.54 mm, reflected light, Normarski interference image of etched surface.

suggest that the columnar impingement microstructure of the orthopyroxene is formed by magmatic crystallization.

Orthopyroxene-spinel symplectite

The orthopyroxene-spinel symplectite forms an irregular, discontinuous layer along the outer contact of the orthopyroxene layer (fig. 5B) and forms plumes that branch outward in the amphibole-spinel symplectite (fig. 7). Spinel is granular in the symplectite layer but occurs as branching colonies of rod-shaped grains in the plumose aggregates. The inner contact of the orthopyroxene-spinel symplectite with orthopyroxene is planar while the outer contact is very irregular. Averaged thickness of the symplectite layer lies in the range 10 to 20 μm . Volume fraction spinel in the symplectite layer is 0.319.

Amphibole-spinel symplectite

Primary amphibole-spinel symplectite consists of fan-shaped grains of pargasite that open toward plagioclase and are ribbed by rods of spinel. Volume fraction spinel in symplectite averages 0.125 ± 0.028 . Although spinel grains appear rod-like in the outer part of the layer and drop-like in the inner part (fig. 5B), the continuity of the spinel rods along amphibole grains is apparent in transmitted light (fig. 5A). Note that the number of amphibole crystals per unit length of layer decreases from the inner contact with orthopyroxene-spinel symplectite to the outer contact with plagioclase. The drop-like appearance of spinel grains in the inner part of the layer is in part due to the poor organization of the columnar impingement microstructure in that part of the

layer. Sections cut through the symplectite roughly parallel to layer contacts show individual amphibole-spinel symplectite colonies to be equant in cross-section and confirm the rod- or thin blade-shape of the spinel grains (fig. 8). Each amphibole-spinel colony is thus cone-shaped and contains 5 to 10 spinel rods within a single grain of amphibole.

The irregular inner contact of the amphibole-spinel layer reflects the highly variable thickness of the orthopyroxene-spinel symplectite layer. Most of the amphibole grains that cross the full width of the symplectite layer appear to have nucleated in embayments in the orthopyroxene-spinel layer. The outer contact of the symplectite layer with plagioclase is characterized by a series of gently curving reaches, convex toward plagioclase and separated by sharp steps, that represent the termini of individual amphibole-spinel colonies.

The individual amphibole-spinel symplectite colonies appear to have grown by columnar impingement at the expense of plagioclase. The irregular nature of the inner contact suggests that growth of the amphibole-spinel symplectite may have been coupled with or may post-date dissolution of the orthopyroxene-spinel symplectite. However, the occurrence of plumose colonies of orthopyroxene-spinel symplectite within parts of amphibole-spinel layers in some coronas, suggests that growth of the two symplectites may have overlapped in time.

The apparent width of the amphibole-spinel symplectite layer can be quite variable from corona to corona, ranging from 110 ± 12 to $205 \pm 2 \mu\text{m}$, but the thickness of the layer on planar reaches of individual coronas is quite uniform. The layer

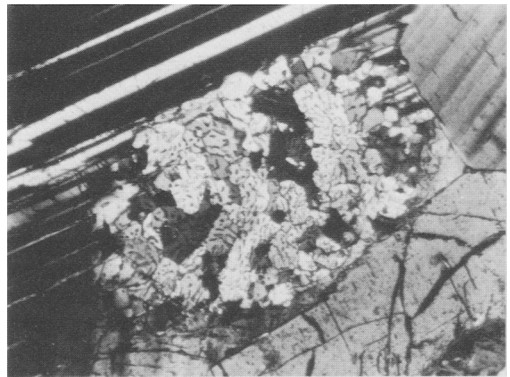


FIG. 8. Primary corona microstructure sectioned through amphibole-spinel symplectite, roughly perpendicular to axis of amphibole-spinel colonies. Width of field, 0.75 mm, crossed polars.

TABLE III
ELECTRON MICROPROBE ANALYSES - ANNEALED CORONA ASSEMBLAGE

	WEIGHT PERCENT OXIDE					
	OL	OPX	AMP-1	AMP-2	AMP-3	PLAG
SiO ₂	37.35	54.02	42.15	41.15	41.87	51.92
TiO ₂	-	-	-	-	-	-
Al ₂ O ₃	-	1.90	16.86	17.53	17.05	31.06
Cr ₂ O ₃	-	-	-	-	-	-
FeO	33.10	18.57	9.21	9.34	8.90	0.12
MnO	0.38	0.33	-	0.14	-	-
MgO	31.03	24.64	14.08	13.29	13.75	-
CaO	0.06	0.31	11.84	11.38	11.66	13.20
Na ₂ O	-	-	2.78	2.67	2.85	3.92
K ₂ O	-	-	0.75	0.87	0.85	-
ΣOXIDES	101.92	99.76	97.67	96.40	96.93	101.23
	MINERAL FORMULA					
Si (4+)	1.003	1.973	6.110	6.051	6.109	2.349
Ti (4+)	-	-	-	-	-	-
Al (3+)	-	0.082	2.881	3.040	2.934	1.657
Cr (3+)	-	-	-	-	-	-
Fe (2+)	0.743	0.568	1.116	1.149	1.085	0.005
Mn (2+)	0.009	0.010	-	0.018	-	-
Mg (2+)	1.241	1.341	3.043	2.913	2.990	-
Ca (2+)	0.002	0.012	1.839	1.793	1.823	0.640
Na (1+)	-	-	0.782	0.755	0.807	0.344
K (1+)	-	-	0.138	0.163	0.158	-
ΣCATIONS	2.997	3.986	15.909	15.894	15.907	4.994
ΣOXYGEN	4	6	23	23	23	8
Mg/Mg+Fe	0.626	0.702	0.732	0.717	0.734	-
Ca/Ca+Na	-	-	0.702	0.704	0.693	0.650
Al/Al+Si	-	0.040	0.320	0.334	0.324	0.414

AMP-1, amphibole from monomineralic layer; AMP-2, amphibole from annealed symplectite; AMP-3, amphibole from primary symplectite

thins around corners and pinches out beyond the ends of olivine grains enveloped by post-cumulus clinopyroxene.

MICROSTRUCTURE OF ANNEALED CORONAS

The microstructure of the annealed corona shown in fig. 4 (bottom) is illustrated in the micrographs of fig. 9A and B and representative electron probe analyses of minerals from this corona are listed in Table III.

The orthopyroxene layer and the amphibole of the amphibole-spinel symplectite of annealed coronas each consist of a single, optically continuous crystal, that may partially or wholly envelop the olivine core (figs. 9A and 10). The orthopyroxene and symplectite layers are separated by a layer of inclusion-free amphibole, optically continuous with the amphibole of the symplectite. Symplectitic spinel occurs in parallel rod-shaped

grains, oriented approximately perpendicular to layer contacts (fig. 9B), with an average volume fraction spinel of 0.133 ± 0.044 . Thus, the annealing process eliminated the low-angle grain boundaries in orthopyroxene and amphibole, spinel rods were rotated into parallel positions, the orthopyroxene-spinel symplectite disappeared and a monomineralic amphibole layer formed separating orthopyroxene and the amphibole-spinel symplectite. All layer contacts are planar or gently curving. Cuspate terminations on olivine grains are rounded and back-to-back layers of orthopyroxene do not occur (fig. 6, upper-right centre).

The corona on a given olivine may be partially or wholly annealed, or it may retain the primary microstructure throughout. Amphibole-spinel symplectite appears to anneal more readily than does the orthopyroxene layer because orthopyroxene locally retains low-angle grain boundaries along segments of the layer in annealed

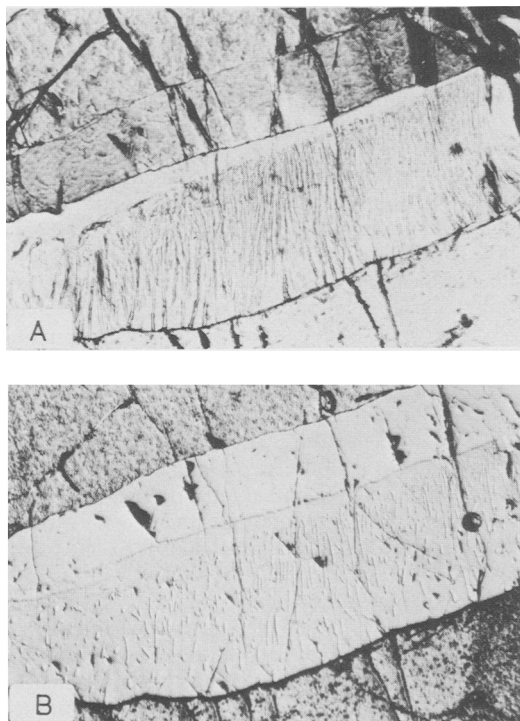


FIG. 9. Annealed corona microstructure of olivine illustrated in fig. 4 (bottom). Olivine (upper left) separated from plagioclase (bottom) by layers comprising a single crystal of orthopyroxene and a single crystal of amphibole. Rods of spinel in outer part of amphibole layer in parallel alignment. Magmatic clinopyroxene separates orthopyroxene and amphibole at left of field and spinel occurs as blebs rather than rods. At right edge of field, annealed microstructure is in contact with primary corona microstructure (fig. 12). Electron probe analyses in Table III are from grains in this field of view. Width of field, 0.54 mm. *A.* Crossed polars. *B.* Reflected light, Normarski interference image of etched surface.

coronas in which all amphibole of the symplectite layer has annealed to a single grain (fig. 10). The occurrence of orthopyroxene-spinel symplectite adjacent to spinel-free amphibole has not been observed. Plumose colonies of orthopyroxene-spinel symplectite may persist along the outer margin of annealed amphibole-spinel symplectite, however.

All olivine grains with coronas that possess the annealed microstructure are partially rimmed by a crystal of inclusion-free, magmatic amphibole in contact with orthopyroxene (fig. 10 top centre, fig. 4, bottom left). Corona amphibole has the same optical orientation as magmatic amphibole, which may serve as a template for annealing. Note,

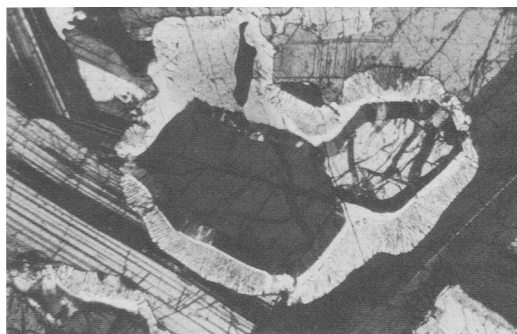


FIG. 10. Annealed corona surrounding two grains of cumulus olivine. Although a single crystal of symplectitic amphibole, optically continuous with magmatic amphibole envelops both olivine grains, orthopyroxene remains incompletely annealed. Width of field, 2.1 mm, crossed polars.

however, that the presence of magmatic amphibole does not appear to be sufficient to cause annealing. In many cases, there is a short lens of magmatic clinopyroxene along a part of the contact between orthopyroxene and amphibole of annealed coronas (fig. 9, left centre).

PHASE COMPOSITION

Energy dispersive electron probe microanalyses were obtained with the electron microprobe designed and built in the Department of Earth Sciences, University of Cambridge (Sweatman and Long, 1969; Statham, 1976), and operated under the supervision of Jim Long and Peter Treloar. Analyses of minerals in the magmatic assemblage and in primary, annealed and oxide coronas are listed in Tables I-IV. The set of analyses in each table is from a single corona of magmatic microstructure. The most remarkable feature of these data is the fact that all phases are compositionally homogeneous at the grain level and there is essentially no compositional variation from grain to grain or microstructure to microstructure.

Olivine

Olivine ranges in composition from FO_{61} to FO_{64} , but individual grains are unzoned. Olivine grains surrounded by coronas tend to have compositions of FO_{62} , but are not systematically depleted in Mg relative to those in the magmatic assemblage.

Orthopyroxene

Orthopyroxene occurs only as rims on olivine in the intercumulus and corona associations. It ranges

TABLE IV
ELECTRON MICROPROBE ANALYSES - OXIDE CORONA ASSEMBLAGE

	WEIGHT PERCENT OXIDE			
	ILM	SP	AMP	PLAG
SiO ₂	0.036	-	41.04	52.03
TiO ₂	53.48	0.18	3.06	-
Al ₂ O ₃	0.09	64.87	16.23	30.67
Cr ₂ O ₃	0.05	0.18	0.05	-
FeO	43.07	21.90	9.94	0.15
MnO	0.40	-	0.02	-
MgO	2.63	13.12	11.95	-
CaO	-	0.03	11.54	13.02
Na ₂ O	-	-	2.83	4.01
K ₂ O	-	-	0.84	-
ΣOXIDES	100.08	100.28	97.50	99.89
	MINERAL FORMULA			
Si (4+)	0.009	-	6.003	2.361
Ti (4+)	0.992	0.004	0.337	-
Al (3+)	0.003	1.998	2.798	1.641
Cr (3+)	0.001	0.004	0.006	-
Fe (2+)	0.888	0.478	1.216	0.006
Mn (2+)	0.008	-	0.003	-
Mg (2+)	0.096	0.511	2.605	-
Ca (2+)	-	0.001	1.808	0.633
Na (1+)	-	-	0.802	0.353
K (1+)	-	-	0.158	-
ΣCATIONS	1.997	2.995	15.737	4.995
ΣOXYGEN	3	4	23	8
Mg/Mg+Fe	0.098	0.517	0.682	-
Ca/Ca+Na	-	-	0.693	0.642
Al/Al+Si	-	-	0.318	0.410

in composition from EN₇₀ to EN₇₂. There is no variation in orthopyroxene composition within corona layers or between coronas, and the composition of orthopyroxene in both primary and annealed coronas is identical to that forming rims separating olivine and clinopyroxene in the magmatic assemblage. The mole fraction Mg of orthopyroxene varies systematically with that of coexisting olivine. Olivine of FO₆₄ in corona cores coexists with orthopyroxene of EN₇₀ in the layer of both primary and annealed coronas. These compositions match those of Medaris's (1969) exchange experiments, indicating that orthopyroxene and olivine are in exchange equilibrium at the layer contact.

Amphibole

Amphibole occurs in five parageneses in the troctolite: (1) as a thin rim separating clinopyroxene and plagioclase in the intercumulus magmatic assemblage, (2) as inclusion-free single crystals associated with clinopyroxene or ilmenite

in what appears to be a magmatic association, (3) in the amphibole-spinel symplectite of the primary coronas on olivine and ilmenite, (4) in the amphibole-spinel symplectite of the annealed coronas on olivine and ilmenite, and (5) in the monomineralic layer separating orthopyroxene or ilmenite and symplectite in annealed coronas. Although amphibole in each of these parageneses has distinct compositional characteristics, amphibole in all associations has a composition close to that of ideal pargasite and the range of compositional variation among all parageneses is less than 3% relative for each cation. Amphibole has a mole fraction Mg of 0.68–0.73. It is slightly enriched in Si and Mg+Fe and depleted in Al, Ca, and Na relative to ideal pargasite. The cation total is about 2% lower than the ideal 16 cations per 23 anhydrous oxygen due to incomplete occupancy of the A-site.

The most significant compositional difference between magmatic amphibole and that in olivine coronas is the high concentration of Ti (0.249–0.264 atoms/23 oxygen) and Cr (0.021–0.024 atoms/23 oxygen) in magmatic amphibole and the virtual absence of these elements in the amphibole of olivine coronas. Because the number of atoms of Si per formula unit is essentially the same in magmatic and coronitic amphibole, the slightly lower concentrations of Al and Mg+Fe in magmatic amphibole reflect partial compensation for Ti and Cr on the sixfold sites. Amphibole rimming ilmenite is compositionally similar to magmatic amphibole, with a somewhat higher concentration of Ti (0.325–0.350 atoms/23 oxygen). Amphibole in olivine coronas is colourless, while that in the magmatic assemblage and rimming ilmenite is pale brown in colour, with the strength of absorption increasing with Ti content. Absorption colour and hence, composition, vary smoothly across amphibole grains in the intercumulus association that are continuous with the amphibole in an annealed corona (fig. 10).

There appears to be small-scale element redistribution in amphibole as a result of annealing of the amphibole-spinel symplectite (Table III). Amphibole in the monomineralic layer is enriched in Mg and Ca and depleted in Al and K while that of the symplectite shows complementary enrichments and depletions relative to amphibole of the primary symplectite in the same corona. Compositional differences between amphibole of the symplectite and one-phase layer are no more than 3% relative and lie within the range of values recorded in amphibole of the magmatic assemblage and primary coronas.

Spinel

Green spinel that occurs in blocky intergrowth with ilmenite, is essentially a spinel-hercynite solid

solution ($X_{Mg} = 0.52$), with Ti and Cr (0.004 atoms each/4 oxygen) as the only significant impurities. Because symplectic spinel occurs as rods 1–2 μm in width, direct analysis with the electron probe was not possible. The analysis of spinel reported in Table II and used in computation of the symplectite compositions listed in Table V was extracted from amphibole-spinel composites by elimination of Si, Ca, Na, and K and removal of Al, Mg, and Fe in the proportion in which they occur in coexisting amphibole. The composition of symplectic spinel obtained by this method, necessarily restricted to the spinel-hercynite join, has mole fraction Mg of 0.455 ± 0.015 . Given the uncertainties attendant with this approach, the difference in mole fraction Mg in magmatic and symplectic spinel may be neither significant nor real.

Symplectite

Modal analyses of symplectite were made by repetitive counting of spinel intercepts on a 100 line micrometer eyepiece on polished thin sections and by similar measurement on photomicrographs. Bulk chemical composition of symplectites, computed using the mode and probe analyses of orthopyroxene or amphibole, and spinel are listed in Table V.

Measured values of the volume fraction spinel in primary amphibole-spinel symplectite range from 0.086 ± 0.055 to 0.152 ± 0.035 . The value chosen for computation of bulk composition is 0.125 ± 0.028 (Table V). Measured values of the volume fraction spinel in annealed symplectite show a narrower range, varying from 0.120 ± 0.057 to 0.143 ± 0.036 on different coronas, with a mean value of 0.133 ± 0.044 . The volume fraction spinel in symplectite of primary and annealed coronas are thus essentially identical within limits of uncertainty of the measurements. Although texturally similar to symplectites on olivine, the volume fraction spinel in symplectite on ilmenite, 0.0625 ± 0.0188 , is significantly lower.

The volume fraction spinel in orthopyroxene-spinel symplectite in primary coronas is 0.319 ± 0.038 . The resulting bulk composition has essentially the same concentrations of Si and Al as primary amphibole-spinel symplectite.

Plagioclase

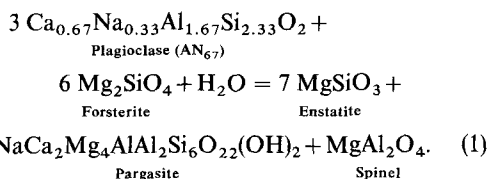
Plagioclase shows no optically discernible zoning and varies in composition from $\text{AN}_{6.4}$ – $\text{AN}_{6.5}$. It has 0.005–0.008 atoms Fe per 8 oxygens. It is characterized by dusting of spinel that imparts a greyish purple colour to the rock in hand specimen.

TABLE V
COMPOSITION OF SYMPLECTITE

	WEIGHT PERCENT OXIDE			
	PRIMARY AMP+SP	ANNEALED AMP+SP	OXIDE AMP+SP	OPX+SP
SiO ₂	36.44	35.75	39.83	35.17
Al ₂ O ₃	24.81	25.71	21.20	23.57
FeO	12.10	12.14	11.49	21.08
MgO	13.53	13.44	12.70	20.09
CaO	10.07	9.90	11.20	0.002
Na ₂ O	2.31	2.30	2.74	-
K ₂ O	0.01	0.01	0.01	-
Σ OXIDES	100.00	100.00	100.00	100.00
	ATOM FRACTION CATION			
	PRIMARY AMP+SP	ANNEALED AMP+SP	OXIDE AMP+SP	OPX+SP
Si (4+)	0.325	0.318	0.356	0.318
Al (3+)	0.261	0.270	0.224	0.250
Fe (2+)	0.090	0.090	0.086	0.159
Mg (2+)	0.180	0.178	0.169	0.270
Ca (2+)	0.096	0.095	0.107	0.002
Na (1+)	0.040	0.040	0.048	-
K (1+)	0.008	0.008	0.009	-
Σ CATIONS	1.000	1.000	1.000	1.000
Σ OXYGEN	1.431	1.428	1.438	1.442
Mg/Mg+Fe	0.666	0.664	0.663	0.629
Ca/Ca+Na	0.706	0.704	0.690	1.0
Al/Al+Si	0.445	0.459	0.386	0.440
	FRACTION SPINEL			
	PRIMARY AMP+SP	ANNEALED AMP+SP	OXIDE AMP+SP	OPX+SP
VOLUME	0.125	0.133	0.062	0.319
MOLE	0.492	0.511	0.326	0.425

CORONA BULK COMPOSITION

Because rims of orthopyroxene and amphibole + spinel everywhere separate olivine and plagioclase in gabbros such as those from Risør, it has long been accepted that such coronas form by reaction between olivine and plagioclase. Such an hypothesis is readily tested by comparison of the proportion of phases measured in coronas with the proportions given by the stoichiometry of the appropriate reaction between olivine and plagioclase. For phase compositions approximating those of the Risør coronas, the corona-forming reaction is



Thus, if the primary or annealed coronas formed by reaction between olivine and plagioclase, their composition should be approximately 7 moles of

TABLE VI
MINERALOGICAL COMPOSITION OF CORONAS

PRIMARY CORONAS				
	OPX	Layer Width [μm]		OPX/AMP+SP
		OPX+SP	AMP+SP	
P1	101 \pm 5	11	205 \pm 5	0.495
P2	72 \pm 13	13 \pm 4	143 \pm 8	0.501
P3	105 \pm 5	17 \pm 4	184 \pm 10	0.570
Moles Mineral				
	OPX	AMP	SP	
P1	5.242	1.0	1.106	
P2	5.549	1.0	1.197	
P3	6.162	1.0	1.204	
ANNEALED CORONAS				
	OPX	Layer Width [μm]		OPX/AMP+SP
		AMP	AMP+SP	
A1	76 \pm 3	19 \pm 5	142 \pm 4	0.538
A2	70 \pm 2	10	124 \pm 4	0.565
A3	76 \pm 5	18 \pm 5	87 \pm 3	0.877
A4	79 \pm 1	18 \pm 2	90 \pm 4	0.881
Moles Mineral				
	OPX	AMP	SP	
A1	4.627	1.0	0.904	
A2	5.145	1.0	0.956	
A3	6.997	1.0	0.802	
A4	7.117	1.0	0.846	

orthopyroxene and 1 mole of spinel per mole of amphibole.

The bulk composition of individual coronas (Table VI) was computed using layer widths measured on linear reaches of corona rims, modal analyses of symplectites (Table V), molar volumes of Mg- and Fe-end member minerals, together with electron probe analyses of corona minerals (Tables II and III). To obtain the true thickness of the mineral assemblage layers of a corona, it is necessary to make measurements on a section cut through its geometrical centre. For coronas with two or more layers, the ratio of the thickness of the innermost layer to that of the outermost layer is a minimum on a corona sectioned through its centre. Measurements on six primary coronas yield values of the ratio of the width of the orthopyroxene layer to that of the amphibole-spinel symplectite layer ranging from 0.495 to 0.867. Similar measurements on four annealed coronas range from 0.538 to 0.881. Only the minimum values of this ratio are considered significant for computation of corona bulk composition. Calculations of the variation in this ratio with distance from the centre of spherical and rectangular coronas indicate that its value does not

differ significantly from that at the centre until the section distance is greater than one-half the radius of the structure. Thus the wide range of values measured may be the result of real variation in the ratio of thicknesses of corona layers.

Measured layer widths and phase proportions, normalized to 1 mole of amphibole, are shown in Table VI for three primary and four annealed coronas. Neither primary nor annealed coronas have compositions that match the stoichiometry of the olivine-plagioclase reaction. Primary coronas (P1 and P2) have 1.1–1.2 moles of spinel and only 5.2–6.6 moles of orthopyroxene per mole of amphibole, while annealed coronas (A1 and A2) have 0.90–0.96 moles of spinel and 4.6–5.1 moles of orthopyroxene.

Although the concentrations of SiO_2 and Al_2O_3 are essentially constant across both symplectite layers of the primary coronas, there is a maximum in the concentration of SiO_2 in the orthopyroxene layer. The concentrations of all other oxides vary in a monotonic, step-wise fashion across the microstructure.

Variation in bulk composition across annealed coronas is essentially the same as that illustrated by Mongkoltip and Ashworth (1983, fig. 6a). The concentration of SiO_2 passes through a minimum in the amphibole-spinel symplectite and rises to a maximum in the orthopyroxene layer, while the concentration of Al_2O_3 decreases in a step-wise fashion from plagioclase to olivine. There are maxima for CaO and Na_2O with corresponding minima for MgO and FeO in the amphibole layer.

DIFFUSION-CONTROLLED GROWTH OF CORONAS IN THE SYSTEM $\text{NaCa}_2\text{O}_{5/2}\text{-MgO-AlO}_{3/2}\text{-SiO}_2$

Stability along gradients in the chemical potentials is a necessary condition for the diffusional growth of a layered structure by solid-state metamorphic processes. Thus the question of whether the Risør coronas developed by metamorphic reaction and diffusional exchange between plagioclase and olivine can be addressed by an analysis of the stability of the mineral assemblage layer sequences of primary and annealed coronas. The stable sequence of mineral assemblage layers developed between incompatible reactants is determined by the relative magnitudes of the instantaneous fluxes of the diffusing components which, in turn, are determined solely by the formulae of the participating phases and the ratios of the Onsager diffusion coefficients (Joesten, 1977). The mineralogical composition of a model corona can be quantitatively simulated by solution of a system of linear mass balance, conservation, and

flux ratio equations describing the diffusion-controlled growth of a radially symmetric model structure (Fisher, 1977; Joesten, 1977). Because the Onsager diffusion coefficients have fixed values at a given temperature and pressure, there is a single mineral assemblage layer sequence that is unique to a given mineral facies. These methods, based on non-equilibrium thermodynamics, have been used to model the diffusion-controlled growth of pyroxene-spinel coronas between olivine and plagioclase by Joesten (1978) and of amphibole-spinel coronas between olivine and plagioclase by Nishiyama (1983).

Diffusional stability in layered structures

If coronas are formed by reaction and subsequent chemical exchange between olivine and plagioclase, the mineral assemblage layers comprising the structures should represent assemblages occupying adjacent volumes in the compositional space of a single mineral facies. Assemblages in local equilibrium across each layer contact buffer the chemical potentials of the exchangeable components and set up potential gradients across the corona. Thus, although the mineral assemblages on either side of a layer contact are in local equilibrium across the boundary, the fact that they lie along a set of chemical potential gradients causes the assemblage of one layer to grow at the expense of that of its neighbour by irreversible reaction with diffusing components. Because each layer-contact reaction consumes and releases components that diffuse down their potential gradients into and away from the reaction site, the identity of reactant and product assemblages and the stoichiometry of the reaction are controlled by the relative diffusive fluxes of components in the adjacent layers. Thus all mineral assemblage layers of the corona grow simultaneously by a set of diffusion-controlled reactions at layer contacts, all of which are linked so that the diffusing components are evolved or consumed in just the proportions needed to balance growth of the overall structure.

In a stable corona structure, mineral assemblage layers grow outward from the initial contact between plagioclase and olivine. Only the layer that contains the initial olivine/plagioclase contact grows by reaction at both contacts. All other layers grow at one contact while being consumed at the other. Because the ratio of the chemical potential gradients within a given layer is determined by the Gibbs-Duhem equations for the constituent phases, the stoichiometry of a given layer contact reaction is determined by the value of the ratio of the Onsager diffusion constants. Thus for a given choice of the Onsager coefficient ratio, a

stable layer contact reaction is one in which the assemblage of the growing layer appears as the product assemblage, while that of the layer being consumed appears as the reactants.

Model system NaCa₂O_{5/2}-MgO-AlO_{3/2}-SiO₂

Diffusion-controlled growth of primary and annealed coronas from Risör is modelled below using the four-component system NaCa₂O_{5/2}-MgO-AlO_{3/2}-SiO₂. Na and Ca are combined as the component NaCa₂O_{5/2} because the mole fraction Ca/(Ca + Na) in this component, 0.67, is the same as that in ideal pargasite and in plagioclase of AN₆₇, while the mole fraction Ca/(Ca + Na) is 0.70 in amphibole and 0.64 in plagioclase in coronas from Risör. For the sake of brevity and to avoid confusion between phases in the model system and the corresponding minerals in the Risör sample, the phases plagioclase, amphibole, spinel, enstatite, and forsterite of the model system will be abbreviated by P, A, S, E, and F, respectively. Thus the layer sequence of the primary coronas is represented as P:A+S:E+S:F, while that of the annealed coronas is given by P:A+S:A:E:F.

The system of mass balance, conservation and flux ratio equations of the type needed to model the growth of primary and annealed coronas is developed in Joesten (1977) and Nishiyama (1983), both of whom provide illustrative examples of their use to which the reader is referred. The system of equations for the annealed corona in the model system is given in Table VII. Solution to the system of equations describing corona growth is obtained by specifying the values of three independent ratios of the four Onsager diffusion coefficients, $L_{\text{NaCa}_2\text{NaCa}_2}/L_{\text{SiSi}}$, $L_{\text{AlAl}}/L_{\text{SiSi}}$, and $L_{\text{MgMg}}/L_{\text{SiSi}}$, and solving for the stoichiometric coefficients for all phases and diffusing components in each of the layer contact reactions. Because the stoichiometric coefficients of the layer contact reactions are sensitive functions of the Onsager coefficient ratios, it is useful to present the results of these calculations on diagrams using these ratios as axes.

Corona growth in the model system

The results of model calculations on coronas in the system NaCa₂O_{5/2}-MgO-AlO_{3/2}-SiO₂ are shown on *L*-ratio diagrams in fig. 11. Onsager coefficients are normalized to the value of L_{SiSi} . It has been found that variation in the ratio $L_{\text{NaCa}_2\text{NaCa}_2}/L_{\text{SiSi}}$ has virtually no effect on the stoichiometry of the layer contact reactions, so results are plotted using $L_{\text{AlAl}}/L_{\text{SiSi}}$ and $L_{\text{MgMg}}/L_{\text{SiSi}}$ at $L_{\text{NaCa}_2\text{NaCa}_2}/L_{\text{SiSi}} = 1$. By using this choice of variables, the effect of variation in the fluxes of two

TABLE VII
SYSTEM OF MASS BALANCE, CONSERVATION AND FLUX RATIO EQUATIONS
FOR CORONAS WITH THE LAYER SEQUENCE P+|A+S-|A|E|-F
IN THE MODEL SYSTEM $\text{NaCa}_2\text{O}_5/2\text{-MgO-AlO}_{3/2}\text{-SiO}_2$

Mass Balance	
P+ A+S	
$v_p^P AS + v_A^P AS + v_{NC}^P AS = 0$	
$4v_A^P AS + v_S^P AS + v_{Mg}^P AS = 0$	
$5v_p^P AS + 3v_A^P AS + 2v_S^P AS + v_{Al}^P AS = 0$	
$7v_p^P AS + 6v_A^P AS + v_{Si}^P AS = 0$	
A+S+ A	
$v_A^A S + v_{NC}^A S = 0$	
$4v_A^A S + v_S^A S + v_{Mg}^A S = 0$	
$3v_A^A S + 2v_S^A S + v_{Al}^A S = 0$	
$6v_A^A S + v_{Si}^A S = 0$	
A -E	
$v_A^A E + v_{NC}^A E = 0$	
$4v_A^A E + v_E^A E + v_{Mg}^A E = 0$	
$3v_A^A E + v_{Al}^A E = 0$	
$6v_A^A E + v_E^A E + v_{Si}^A E = 0$	
E -F	
$v_E^E F + 2v_F^E F + v_{Mg}^E F = 0$	
$v_E^E F + v_F^E F + v_{Si}^E F = 0$	
Conservation	
$v_{NC}^P AS + v_{NC}^A S + v_{NC}^A E = 0$	
$v_{Mg}^P AS + v_{Mg}^A S + v_{Mg}^A E + v_{Mg}^E F = 0$	
$v_{Al}^P AS + v_{Al}^A S + v_{Al}^A E + v_{Al}^E F = 0$	
$v_{Si}^P AS + v_{Si}^A S + v_{Si}^A E + v_{Si}^E F = 0$	
Flux Ratio	
A+S-Layer	
$v_{NC}^P AS [L_{Si}/L_{NC}] - 5v_{Al}^P AS [L_{Si}/L_{Al}] + 6v_{Si}^P AS = 0$	
$2v_{Al}^P AS [L_{Mg}/L_{Si}] + v_{Mg}^P AS [L_{Al}/L_{Si}] = 0$	
A-Layer	
$(v_{NC}^A S + v_{NC}^A A) [L_{Si}/L_{NC}] + 4(v_{Mg}^A S + v_{Mg}^A A) [L_{Si}/L_{Mg}] + 3(v_{Al}^A S + v_{Al}^A A) [L_{Si}/L_{Al}] + 6(v_{Si}^A S + v_{Si}^A A) = 0$	
E-Layer	
$v_{Mg}^E F + v_{Si}^E F [L_{Mg}/L_{Si}] = 0$	
Mineral Formulae	
Plagioclase	$\text{NaCa}_2\text{Al}_5\text{Si}_7\text{O}_{24}$
Amphibole	$\text{NaCa}_2\text{Mg}_4\text{Al}_1\text{Al}_1\text{Si}_6\text{O}_{22}(\text{OH})_2$
Spinel	MgAl_2O_4
Enstatite	MgSiO_3
Forsterite	Mg_2SiO_4
Solve by choosing $[L_{NC}/L_{Si}]$, $[L_{Al}/L_{Si}]$ and $[L_{Mg}/L_{Si}]$ and setting $v_p^P AS = -1$.	

components that diffuse in the same direction, $\text{AlO}_{3/2}$ and SiO_2 , is readily compared with variation in the fluxes of two components that diffuse in opposite directions, MgO and SiO_2 . It should be emphasized that the L -ratios do not represent independent and dependent variables in the usual sense, in that the full range of possible values shown on fig. 11 are not accessible to the system. At a given temperature and pressure, the values of each of the Onsager coefficients is independently determined by the thermally activated diffusion behaviour of each component. Hence their ratios have specific values, so that behaviour of the model system is described by a point on the L -ratio diagram.

In all cases it has been assumed that the system is closed to diffusion beyond the layer contacts with plagioclase and with olivine. Thus all transported material is derived ultimately from the breakdown of plagioclase and forsterite. As a result the overall stoichiometry of all layer contact reactions sums to that of reaction (1).

There are a large number of different ways in which the enstatite, amphibole, and spinel produced by reaction between forsterite and plagioclase can be arranged in a set of mineral assemblage layers that relax the chemical potential gradients between reactant phases and which do not violate conditions of local equilibrium. However, only a small subset of these meet the conditions of diffusional stability (Frantz and Mao, 1975).

The six stable corona types that can be produced by reaction (1) are shown on the L -ratio diagram of fig. 11A. Each is stable over a characteristic range of L -ratios, but since the L -ratios have unique values at a given T and P , only one of the corona types is truly stable in the mineral facies defined by the product assemblage of reaction (1). If the mineral assemblage layer sequence of an observed corona is not stable, then that corona cannot have been produced by any solid-state process. Because the Onsager diffusion constants have unique values at a given temperature and pressure the modes and layer widths measured in coronas can be used to determine the ratios of the instantaneous diffusive fluxes during growth and the ratios of the Onsager diffusion coefficients for the system.

A layer of orthopyroxene in contact with olivine and a layer of amphibole-spinel symplectite in contact with plagioclase are common to both primary and annealed coronas. Textural relations in the primary coronas indicate that orthopyroxene grew at the expense of olivine and that symplectite grew at the expense of plagioclase.

Each of the six corona types in the model system is characterized by a layer of monomineralic enstatite in contact with forsterite. The enstatite

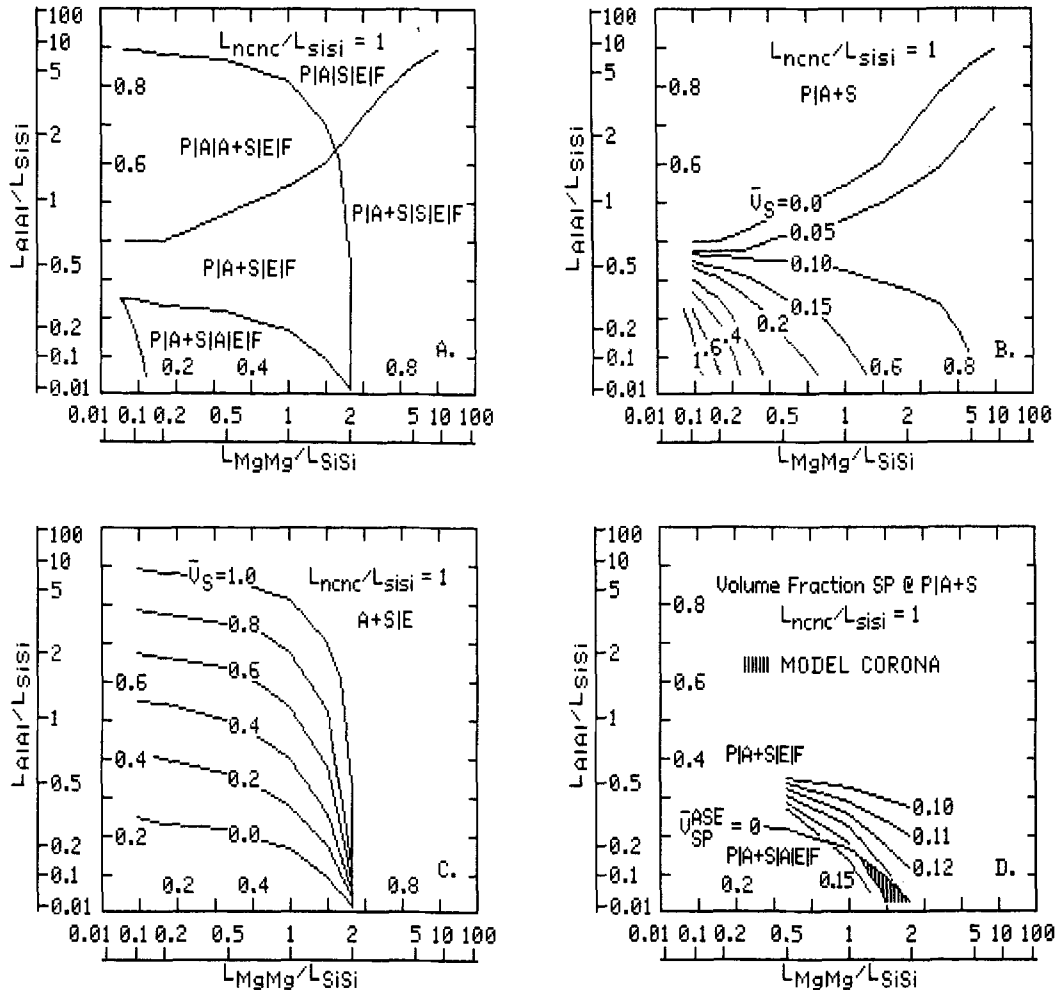
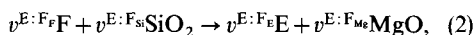


FIG. 11. Corona growth in the model system $\text{NaCa}_2\text{O}_{5/2}\text{-MgO-AlO}_{3/2}\text{-SiO}_2$ as a function of Onsager diffusion coefficient ratios for $\text{AlO}_{3/2}$ (L_{AlAl}), MgO (L_{MgMg}), $\text{NaCa}_2\text{O}_{5/2}$ (L_{ncnc}), and SiO_2 (L_{SiSi}). Phase abbreviations P (plagioclase AN_{67}), A (pargasite), S (spinel), E (enstatite), and F (forsterite). Curves plotted on axes scaled as $L_{\text{AlAl}}/(L_{\text{AlAl}} + L_{\text{SiSi}})$ and $L_{\text{MgMg}}/(L_{\text{MgMg}} + L_{\text{SiSi}})$. (A) Stability fields of corona layer sequences bounded by curves along which volume fraction spinel (V_S) is either zero or one in amphibole-spinel symplectite produced by reaction with plagioclase or enstatite. Stability field of layer sequence P:S:A:E:F at lower left corner. (B) Contours of volume fraction spinel in A+S formed at contact with plagioclase. (C) Contours of volume fraction spinel in A+S formed at contact with enstatite. (D) Stability field of annealed coronas (shaded), bounded by curves for volume fraction spinel at P:A+S equal to 0.12 and 0.14 and curve for volume fraction spinel at A+S:E equal to zero.

layer grows at the expense of forsterite by a reaction of the form



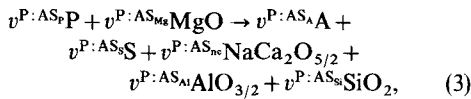
where $v^{\text{E:F}}$ and $v^{\text{E:F}_s}$ represent the stoichiometric coefficients for forsterite and SiO_2 in the irreversible reaction at the E:F layer contact. Forsterite is the ultimate source of all MgO in the phases of the model corona.

The six corona types in the model system (fig. 11A) differ in the distribution of amphibole and spinel, which may occur together in symplectite or individually as monomineralic layers. Note that the model does not predict the texture of two-phase layers. It is assumed that the composition of the two-phase A+S layer is an accurate analogue of the symplectite of the Risør coronas.

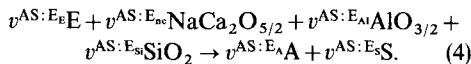
Because the model system is closed to diffusion

beyond the layer contacts with plagioclase and with forsterite, solution to the system of mass balance, conservation and flux ratio equations describing corona growth obtained by setting the value of $v^{P:ASr} = -3.0$ (note that in Table VII, the formula of plagioclase of AN₆₇ is based on 24 oxygens, so that the corresponding value of $v^{P:ASr}$ is -1.0), results in consumption of 6 moles of forsterite and a product assemblage consisting of 7 moles of enstatite and 1 mole each of amphibole and spinel to fit the stoichiometry of reaction (1). In coronas with the layer sequence P:A+S:E:F, symplectite grows at the expense of both P and E, so that 1 mole of A and 1 mole of S are distributed between the parts of the symplectite layer that grew at each contact. In coronas with a layer of A+S and a monomineralic layer of either A or S, 1 mole of A and 1 mole of S are distributed between symplectite and the single-phase layer.

To understand the relation between stable corona layer sequence and values of the Onsager diffusion constants, it is useful to examine variation in the composition of A+S symplectite formed at P:A+S and A+S:E as a function of L -ratio (fig. 11B and C). The growth of A+S at the layer contact with plagioclase is described by the reaction,



while growth of A+S at the layer contact with enstatite is described by the reaction,



Variation in the stoichiometric coefficients of the product phases in reactions (3) and (4) as a function of L -ratio is conveniently expressed in terms of the mole fraction or volume fraction spinel in the A+S assemblage.

Contours of the volume fraction spinel in symplectite (V_S) formed at the contact with plagioclase are shown on fig. 11B and at the contact with enstatite are shown on fig. 11C. A layer of A+S symplectite grows stably at the expense of plagioclase at P:A+S in the region of the L -ratio diagram of fig. 11B bounded by the curves labelled $V_S = 0$ and $V_S = 1$. Similarly, a layer of A+S symplectite grows at the expense of enstatite at A+S:E in the region of fig. 11C bounded by the curves labelled $V_S = 0$ and $V_S = 1$.

Where $V_S = 1$ in the product assemblage of reaction (3) or (4), $v_A = 0$ and a monomineralic layer of spinel grows by reaction with either plagioclase or enstatite. Similarly, where $V_S = 0$, $v_S = 0$ and a monomineralic layer of amphibole

grows at that layer contact. Thus the contours of $V_S = 0$ and $V_S = 1$ define the limit of stability of the P:A+S and A+S:E layer contact assemblages. For values of the L -ratios that lie outside the $V_S = 1$ contour on the P:A+S or A+S:E field, the value of $v_A < 0$ in reaction (3) or (4) and the P:A+S or A+S:E layer contact is unstable.

The L -ratio diagram of fig. 11A is partitioned into six fields by the four curves along which V_S equals either zero or one in P:A+S and A+S:E. Each field is characterized by a corona type. Thus the field of stability of model coronas with the layer sequence P:A+S:E:F is bounded by the field for the corona type P:A+S:A:E:F along $V^{AS:E_S} = 0$, by the field for P:A+S:S:E:F along $V^{AS:E_S} = 1$ and by the field for P:A:A+S:E:F along $V^{P:AS_S} = 0$. A model corona with P:S:A+S:E:F is not stable.

Control of symplectite composition by L_{AlAl} , L_{MgMg} , and L_{SiSi}

Within the field of stability of A+S symplectite in the model system, the volume fraction spinel in A+S varies systematically with L_{AlAl}/L_{SiSi} and L_{MgMg}/L_{SiSi} . The P:A+S layer contact assemblage is stable for essentially all values of L_{MgMg}/L_{SiSi} , but is unstable at high values of L_{AlAl}/L_{SiSi} (fig. 11B). The A+S:E layer contact assemblage is stable for $L_{MgMg}/L_{SiSi} < 2$, for values of L_{AlAl}/L_{SiSi} in the range 0.2–10 (fig. 11C).

For $L_{MgMg}/L_{SiSi} < 2$, $V^{AS:E_S}$ systematically increases from zero at $L_{AlAl}/L_{SiSi} = 0.2$ to unity at $L_{AlAl}/L_{SiSi} = 10$. As L_{AlAl}/L_{SiSi} increases, the flux of $AlO_{3/2}$ into the A+S:E layer contact increases relative to that of SiO_2 , so that an Al-rich, hence spinel-rich, assemblage grows at the expense of enstatite. At fixed L_{AlAl}/L_{SiSi} , $V^{AS:E_S}$ systematically increases with increasing L_{MgMg}/L_{SiSi} because the flux of $AlO_{3/2}$ into the A+S:E layer contact is greater than that of SiO_2 . For $L_{MgMg}/L_{SiSi} > 2$, the flux of SiO_2 into the layer contact with enstatite is too small relative to that of $AlO_{3/2}$ reaching the contact or of MgO leaving the contact, to allow formation of amphibole in addition to spinel.

The volume fraction spinel at P:A+S decreases as L_{AlAl}/L_{SiSi} increases, in a way that is sympathetic to that at A+S:E, but does not exactly balance it. As L_{AlAl}/L_{SiSi} increases at fixed L_{MgMg}/L_{SiSi} , the flux of $AlO_{3/2}$ out of the P:A+S layer contact is greater than that of SiO_2 , so that an Al-poor, hence Si- and amphibole-rich layer forms at the contact with plagioclase. This effect is further illustrated by the sequence of corona types that are encountered along a path of increasing L_{AlAl}/L_{SiSi} at fixed L_{MgMg}/L_{SiSi} (fig. 11a).

Note that over much of their range, contours of volume fraction spinel are roughly parallel the L_{MgMg}/L_{SiSi} axis. This is because the main effect of variation in the fluxes of two components that diffuse in the same direction is to separate those components by producing either two A+S symplectite layers with different modes, by segregation of A and S into symplectite and a monomineralic layer or by segregation of A and S into two monomineralic layers (Joesten, 1977). The effect of differences in the fluxes of two components that diffuse in opposite directions is to control the fraction of the width of the layers made up of A and S that grow at the contacts with plagioclase and with enstatite. For example, as L_{MgMg}/L_{SiSi} is increased at $L_{AlAl}/L_{SiSi} = 0.5$, there is very little variation in the volume fraction of spinel in symplectite at P:A+S or A+S:E, but the amount of symplectite formed at P:A+S steadily increases while the amount formed at A+S:E decreases. Variation in L_{MgMg}/L_{SiSi} determines the fraction of the three moles of reactant plagioclase that is used to form A+S at the P:A+S layer contact and the fraction that is converted to $NaCa_2O_{5/2}$, $AlO_{3/2}$, and SiO_2 that diffuse down their gradients to the contact with enstatite to contribute to the growth of A+S at that layer contact.

Primary coronas in the model system and in the Risör sample

The layer sequence corresponding to that of the primary coronas, P:A+S:E+S:E:F, is not stable in the model system. Indeed, there are no stable corona types with the two-phase assemblage, enstatite+spinel. It is highly unlikely that the apparent instability of the primary corona is a result of any of the simplifications introduced either in development of the model (Joesten, 1977) or in a reduction in number of components to simulate the Risör sample. Apart from the absence of a stability field for the primary corona layer sequence on the L-ratio diagram for the model system, there are a number of microstructural features of the primary coronas from Risör that are inconsistent with growth of the corona layers by motion away from the initial contact between reactant plagioclase and olivine.

Amphibole-spinel symplectite colonies in the Risör sample fan outward into plagioclase, consistent with growth of the amphibole-spinel layer at the expense of plagioclase. Similarly, the columnar impingement microstructure of the orthopyroxene layer is consistent with growth of the orthopyroxene at the expense of olivine. However, plumose colonies of orthopyroxene-spinel symplectite within the amphibole-spinel layer are

difficult to reconcile with growth of the corona by reaction between olivine and plagioclase.

Comparison of the direction of motion of the interior layer contacts in the primary coronas as predicted by models for multicomponent-multiphase diffusion and by interpretation of microstructures leads to contradictory results. Frantz and Mao (1975) have shown that where a one-phase and a two-phase layer in contact share a phase in common, the monomineralic layer grows at the expense of the two-phase layer by dissolution of the singular phase. The validity of this relation is independent of the assumption that diffusion is closed beyond the contacts of the reaction band. Thus, in a model corona with the layer sequence P:A+S:E+S:E:F, the enstatite layer of the primary coronas is predicted to grow at the expense of the enstatite-spinel symplectite. Because the enstatite layer would then grow at both contacts, the enstatite-spinel layer would have to grow at the expense of the amphibole-spinel layer. This leads to two problems. First, the irregular contact between the two symplectite layers in the Risör coronas and the discontinuous nature of the orthopyroxene-spinel layer suggest that it is being dissolved rather than growing at its contact with the amphibole-spinel layer. Second, if amphibole were broken down at the layer contact with orthopyroxene+spinel, it is difficult to account for the $NaO_{1/2}$, CaO and $AlO_{3/2}$ released. There is no mineralogical sink for these components in the interior of the corona and they cannot diffuse up-gradient to the layer contact with plagioclase. In addition, the initial contact between olivine and plagioclase would lie within the orthopyroxene layer. Breakdown of sufficient plagioclase to supply SiO_2 for both symplectite layers and orthopyroxene would leave an excess of $AlO_{3/2}$ and $NaCa_2O_{5/2}$ over that needed to form amphibole and spinel.

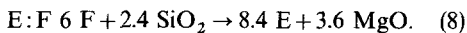
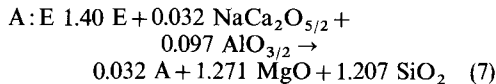
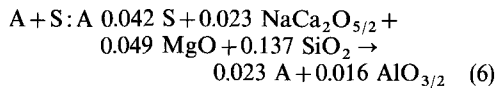
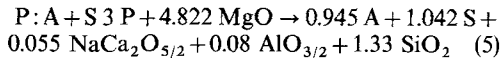
The significance of the instability of the primary corona layer sequence in the model system P:A+S:E+S:E:F is that, irrespective of how it formed, it should spontaneously transform to a stable layer sequence with consequent redistribution of components.

Annealed coronas in the model system and in the Risör sample

The mineral assemblage layer sequence of the annealed coronas from Risör has a direct analogue in the model system. Model coronas with the layer sequence P:A+S:A:E:F are stable for values of L_{MgMg}/L_{SiSi} in the range 0.1 to 2 and for L_{AlAl}/L_{SiSi} less than about 0.2 (fig. 11A). Measured values of the volume fraction spinel in amphibole-spinel symplectite in annealed coronas lie in the range

0.12–0.14. Thus the values of the L -ratios defined by the layer sequence and symplectite composition of Risør annealed coronas must simultaneously lie between the curves for $V^{P:AS_s} = 0.12$ and 0.14 and at L_{AlAl}/L_{SiSi} lower than those defined by the curve for $V^{AS:Es} = 0$. The shaded area on the L -ratio diagram of fig. 11D shows that the Risør annealed coronas constrain the value of L_{AlAl}/L_{SiSi} to be less than 0.15 while that of L_{MgMg}/L_{SiSi} must lie between 1 and 2.

The system of linear mass balance, conservation and flux ratio equations that describe growth of coronas with the layer sequence P:A+S:A:E:F in the model system is given in Table VII. The following set of layer contact reactions obtained by solving the system of equations of Table VII for $L_{nnc}/L_{SiSi} = 1$, $L_{AlAl}/L_{SiSi} = 0.05$ and $L_{MgMg}/L_{SiSi} = 1.5$ describe growth of an annealed corona in the model system:



Note that the stoichiometric coefficients of each of the transported components in reactions (5)–(8) sum to zero and the overall stoichiometry of the set of layer contact reactions is that of reaction (1).

Comparison of the mole proportions of minerals in the model corona, 7 moles E, 1 mole A and 1 mole S, with those in the annealed coronas from Risør (Table VI), 4.627 mole orthopyroxene and 0.904 mole spinel per mole of amphibole shows that coronas from the natural system have too little orthopyroxene and spinel relative to amphibole. The composition of the model coronas is that which results from exchange of components from the breakdown of 3 moles plagioclase and 6 moles of forsterite. However, the Risør annealed coronas formed by annealing of pre-existing primary coronas that cannot have been formed by the olivine–plagioclase reaction. Thus the bulk composition of the annealed coronas is largely inherited. Any net layer growth on annealing must take place in the proportions given by reactions (5)–(8), however.

Although analysis of the model system does not contribute to understanding of why some coronas are wholly or partially annealed while others retain the primary microstructure, it does show that

annealing is the result of the diffusional instability of the primary corona layer assemblage sequence.

MASS TRANSFER IN THE ANNEALING PROCESS

The stoichiometry of reactions (5)–(8) gives the mass transfer for the growth of an annealed corona by reaction between plagioclase (AN_{67}) and forsterite in the model system. Analogous results can be obtained for the real system using electron probe analyses of minerals (Table III) and symplectite composition (Table V) for the Risør coronas. The problem of calculating the mass transfer involved in the growth of the mineral assemblage of a given layer at the expense of its neighbour is that of obtaining a solution to a system of mass balance equations like those in Table VII. Mass balance for each layer contact is obtained independently, because conservation and flux ratio constraints are not applied. Thus it is necessary to make an arbitrary choice of reference frame against which to measure gains and losses to the system and to fix the amount of either product assemblage formed or reactant assemblage consumed.

Calculation of the mass balance at a layer contact is readily done using the method of Gresens (1967) who has shown that the number of moles of each component evolved or consumed on the growth of one assemblage at the expense of another varies linearly with the ratio of the volume of the product assemblage formed to the volume of the reactant assemblage consumed. This ratio, called the volume factor, f_v , has a value of unity for a volume-fixed frame, and is greater than or less than one when there is a net increase or decrease in volume in the layer contact reaction. Its value can be chosen so as to conserve any one component. The number of moles of component i consumed ($v_i < 0$) or evolved ($v_i > 0$) on the conversion of assemblage A to assemblage B is given by

$$v_i = -\{[f_v(V^A/V^B)n_i^B] - n_i^A\}, \quad (9)$$

where V^A and V^B are the volumes per mole of assemblages A and B and n_i^A and n_i^B are the number of moles of component i per formula unit of assemblages A and B. Thus the value of v_i is the number of moles of component i added to (–) or removed from (+) 1 mole of assemblage A on conversion to $f_v(V^A/V^B)$ moles of assemblage B.

There have been many attempts to calculate the stoichiometry of corona-forming reactions and to obtain a net mass balance for the growth of coronas by chemical exchange between olivine and plagioclase. The volume-fixed frame has been used by Reynolds and Frederickson (1962), Grieve and

TABLE VIII
MASS TRANSFER FOR GROWTH OF ANNEALED CORONAS

	P \leftrightarrow A+S		A+S \leftrightarrow A		A \leftrightarrow E		E \leftrightarrow F		NET BALANCE	
	Model	Risör	Model	Risör	Model	Risör	Model	Risör	Model	Risör
Plagioclase	-3.0	-3.0	-	-	-	-	-	-	-3.0	-3.0
Amphibole	0.945	0.942	0.023	0.023	0.032	0.032	-	-	1.0	0.997
Spinel	1.042	0.985	-0.042	-0.058	-	-	-	-	1.0	0.925
Orthopyroxene	-	-	-	-	-1.4	-1.4	8.4	8.453	7.0	7.053
Olivine	-	-	-	-	-	-	-6.0	-6.0	-6.0	-6.0
SiO ₂	1.33	1.34	-0.137	-0.143	1.207	1.184	-2.4	-2.321	0	0.06
AlO _{3/2}	0.08	0.134	0.016	0.011	-0.097	-0.036	-	-0.347	0	-0.238
FeO	-	-1.606	-	-0.004	-	0.362	-	2.057	-	0.809
MgO	-	-3.195	-	-0.050	-	0.841	-	1.778	-	-0.626
*MgO	-4.822	-4.801	-0.049	-0.054	1.271	1.203	3.6	3.835	0	0.183
CaO	0.11	0.227	-0.046	-0.042	-0.064	-0.051	-	-0.039	0	0.056
NaO _{1/2}	0.055	0.32	-0.023	-0.018	-0.032	-0.025	-	-	0	0.277
KO _{1/2}	-	-0.155	-	-0.004	-	-0.004	-	-	-	-0.163
Volume Factor	0.9881		1.382		0.1984		1.0005			

Gittins (1975) and by van Lamoen (1979) while an Al-fixed frame was used by Whitney and McLelland (1973) and McLelland and Whitney (1977, 1980a and b) and an Al- and Si-fixed frame was used by Mongkoltip and Ashworth (1983). In each case the authors suggested compelling reasons for what is necessarily an arbitrary choice, while in each case satisfactory mass balance for all components was not achieved. There are a number of reasons for these failures. First, calculations for model structures, such as that of the annealed corona [reactions (5)–(8)], make it clear that neither volume nor a single component can be conserved at all layer contacts (see also Joesten, 1977). Second, all mass balance calculations require assumptions about which layer contacts involve reaction and about the identity of the reactant and product assemblages. Most importantly, however, it is apparent that the bulk composition of the corona layers is not derived solely from the products of the breakdown of plagioclase and olivine (van Lamoen, 1979; Mongkoltip and Ashworth, 1983).

The first two pitfalls can be avoided by using the results of calculations in the model system [reactions (5)–(8)] as a guide for the choice of a reference frame for each layer contact and for identifying the direction of motion of the interior layer contacts. Mass balances were obtained for each layer contact in the annealed corona using the analytical data in Tables III and V with volume factors calculated from the stoichiometry of the corresponding reactions in the model system. Results of the mass balance calculations for the Risör annealed coronas are compared with the stoichiometry of the corresponding reactions in the

model system in Table VIII. It should be pointed out that the mass balance calculations in Table VIII only attempt to match the stoichiometry of the layer contact reactions. Although the amount of reactant assemblage consumed was chosen to match the stoichiometry of reactions (5)–(8) in the model system, these calculations do not make use of the measured layer widths. It should be recalled (Table VI) that the measured phase proportions of annealed coronas do not match those of reaction (1).

The correspondence between the model system and Risör coronas, both for individual layer contacts and for the net mass balance, is good for amphibole, orthopyroxene, SiO₂ and FeO + MgO (denoted as *MgO). The imbalance in CaO and NaO_{1/2} is largely due to the fact that Risör amphibole is deficient in these components relative to ideal pargasite (Table III) while the imbalance in AlO_{3/2} is largely due to the presence of Al in orthopyroxene. There is no source for potassium among the reactant phases in either the model or the natural system. Balance for individual components is extremely sensitive to actual phase composition. Much of the imbalance in *MgO and SiO₂ at the orthopyroxene/olivine contact is eliminated by normalization of probe analyses of orthopyroxene and olivine to 2.0 cations in the sixfold sites.

The Fe–Mg imbalance for the net corona (Table VIII) has plagued all previous attempts to obtain a mass balance for coronas using olivine and plagioclase as reactants. Because olivine and orthopyroxene are in Fe–Mg exchange equilibrium at the layer contact (see also van Lamoen, 1979, fig. 6)

that is the source of the exchangeable components, the mole fraction Mg in orthopyroxene is not diffusion-controlled. The unequal partitioning of Fe and Mg between olivine and orthopyroxene virtually precludes a net balance for these components over the whole structure if equilibrium partitioning occurs. A net balance for FeO and MgO should be attained if the partitioning of these components between orthopyroxene and amphibole and between amphibole and spinel is diffusion-controlled. The fact that a balance is not achieved has led previous workers to postulate sources and sinks for these components external to the corona and with the requisite transport and exchange via a fluid.

Although the composition of the model corona is readily obtained using material derived solely from the breakdown of plagioclase and forsterite, all attempts to obtain a net mass balance for the growth of natural coronas, including the present one, have failed. The closed system assumption works for the model system but fails for actual corona compositions. The instability of the primary corona layer sequence in the model system suggests that the bulk composition of the corona is not the result of diffusive exchange of material along potential gradients between plagioclase and olivine. The utility of the calculations presented here is that if there is significant growth of corona layers in the annealing process, the results in Table VIII indicate the proportions in which components are exchanged at each layer contact.

Although the choice of a reference frame is arbitrary, the choice is usually made on the basis of the observed or perceived behaviour of the system. Coronas neither deform enveloping plagioclase nor enclosed olivine, so the assumption that replacement at constant volume has seemed reasonable. Volume factors for growth of the amphibole-spinel symplectite at P:A+S and of orthopyroxene at E:F are 0.9887 and 1.0005, respectively. Because the symplectite and orthopyroxene layers comprise 95% of the volume of an annealed corona, the constant volume assumption of earlier workers was indeed a good approximation to reality. Note, however, that volume factors at the interior layer contacts depart significantly from unity and that the total volume change for corona growth in the model system, 16.7%, is equal to ΔV for the solids in reaction (1).

MICROSTRUCTURAL EVOLUTION

Adherence to the ruling paradigm for metamorphic corona growth has caused recent authors to emphasize the regularity of development of corona layers along contacts between olivine and

plagioclase. There are, however, a large number of textural and compositional features in the primary coronas from Risør that are inconsistent with an origin by reaction between olivine and plagioclase. These features, described above, are summarized here for each layer and layer contact.

Interpretation of critical microstructures of primary coronas

1. Cuspate olivine/orthopyroxene contacts are inconsistent with diffusion-controlled reaction. Strongly curved orthopyroxene/olivine contacts on some primary coronas are convex toward olivine and terminate in a cusp, suggestive of extensive loss by reaction or dissolution (fig. 6). Similar cuspate contacts are developed between ilmenite and amphibole-spinel symplectite (fig. 3). Diffusion-controlled growth of orthopyroxene at the expense of a polyhedral grain of olivine should lead to rounding off of corners and preservation of planar faces.

Experimental dissolution of euhedral crystals of forsterite in a melt of peritectic composition in the system diopside-forsterite-silica (Kuo and Kirkpatrick, 1985) leads to a rounding of grain corners and a contact between forsterite and melt that is convex toward forsterite. It should be noted, however, that these experiments were of short duration (< 1 hour) and involved a net decrease in radius of the order of 10% (100 μm). Because the solid/melt interfaces are convex toward the dissolving grain, continued dissolution should produce cusps at their intersection. Cuspate olivine grains are thus inconsistent with diffusion-controlled growth of the orthopyroxene layer but are consistent with dissolution of olivine in melt.

2. Geometry of the columnar impingement orthopyroxene layer on cuspate olivine is inconsistent with diffusion-controlled growth. The layer of columnar impingement orthopyroxene maintains uniform thickness where it wraps around non-cuspate corners on olivine in primary coronas (figs. 1 and 4). Where layers meet at a cusp, they continue past the cusp with their inner margins in contact and terminate along a planar surface (fig. 6). Diffusion-controlled growth of layers around an irregular core grain should involve a thickening of inward-growing layers and a thinning of outward-growing layers where they wrap around corners. Thus, growth of the orthopyroxene layer by diffusion-controlled reaction with olivine should lead to a thickening of the layer at corners that is not observed. It should be noted that the amphibole-spinel symplectite layer thins around corners as expected (figs. 1, 4, 6, and 12A).

3. Columnar impingement orthopyroxene

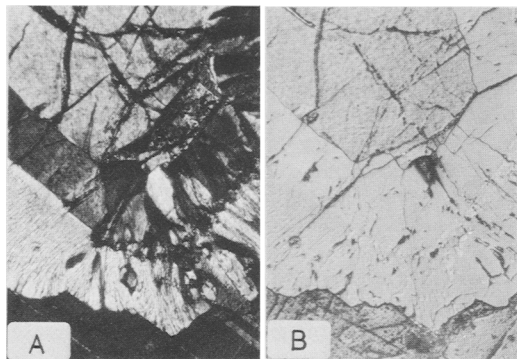


FIG. 12. Transition along strike of corona layers from primary microstructure (right) to annealed microstructure (left) on olivine illustrated in figs. 4 and 9. Olivine (top) rimmed by orthopyroxene and amphibole-spinel symplectite. Width of field, 0.35 mm. *A*. Crossed polars. *B*. Reflected light, Normarski interference image of etched surface.

separates grains of cumulus and intercumulus phases. Although the orthopyroxene layer with the radial microstructure is characteristic of the primary coronas, it has been observed separating olivine and intercumulus amphibole in the magmatic association (see also Brögger, 1934, figs. 37–40) and separating grains of cumulus olivine. In the latter association, a single columnar impingement layer is developed between the two olivine grains; thus it cannot be the result of sectioning through coronas on adjacent olivines. In the examples illustrated by Brögger (1934, figs. 38 and 39), the olivines separated by a rim of radial orthopyroxene are enveloped by intercumulus amphibole, and no symplectite is present. These two textural associations, which strongly imply that columnar impingement orthopyroxene is magmatic in origin, are relatively common.

4. Orientation of cumulus plagioclase laths appears to have been controlled by cusped shape of cumulus olivine. The contacts between cumulus plagioclase laths in contact with coronas developed on cusped olivine grains commonly strike directly into the cusp. The outer contact of the orthopyroxene layer is parallel to the inner contact, preserving the irregular shape of the olivine. Plagioclase laths appear to have been fitted around the irregularly shaped orthopyroxene-rimmed cumulus olivine. These textural relations suggest that cumulus plagioclase came into contact with cumulus olivine, rimmed by orthopyroxene, either during or after orthopyroxene crystallization.

5. Columnar impingement orthopyroxene occurs in contact with plagioclase. In a single

instance, a blade of orthopyroxene extending from the columnar impingement rim on olivine, cross-cuts the layer of amphibole-spinel-symplectite which pinches out against it on either side. The orthopyroxene forms a narrow, V-shaped wedge between two laths of cumulus plagioclase.

Taken together with the textures described in the intercumulus magmatic association, the observations summarized in sections 3, 4, and 5 clearly show that the orthopyroxene rim on olivine is magmatic in origin. Because olivine is found only in contact with orthopyroxene, it is likely that olivine and plagioclase were never in contact.

6. Apparent direction of motion of the orthopyroxene-spinel/amphibole-spinel layer contact is inconsistent with simultaneous diffusion-controlled growth of orthopyroxene-spinel and amphibole-spinel layers. The irregular contact between the orthopyroxene-spinel and amphibole-spinel layers and that fact that the former is locally missing along that contact (fig. 5B), suggest that the orthopyroxene-spinel symplectite layer was being dissolved at its outer contact. The columnar impingement microstructure of the amphibole-spinel symplectite colonies clearly shows that its growth was unidirectional, at the expense of plagioclase (fig. 5A). Thus, dissolution of the orthopyroxene+spinel layer cannot have been the result of the inward growth of the amphibole+spinel layer.

Analyses of diffusion-controlled layer growth in multicomponent-multiphase systems show that the layer contact between a monomineralic layer and a two-phase layer that share a phase in common is unstable and that the monomineralic layer grows by consumption of the phase that is unique to the two-phase layer (Frantz and Mao, 1975; Joesten, 1977, fig. 7). Thus, if the primary corona microstructure evolved by diffusion-controlled reaction between olivine and plagioclase, the orthopyroxene layer should have grown at the expense of the orthopyroxene-spinel layer, which in turn, would have grown at the expense of the amphibole-spinel layer. The textural relations at the orthopyroxene-spinel/amphibole-spinel layer contact clearly do not support this hypothesis. Textural relations at the orthopyroxene/orthopyroxene+spinel layer contact are not as clear cut. Although the very small grain size of spinel (1–5 μm) makes observation difficult, spinel grains in the orthopyroxene-spinel symplectite appear to be tangential to the contact with the orthopyroxene layer, rather than being truncated as expected had that contact moved outward as a result of diffusion-controlled reaction.

7. Plumose orthopyroxene-spinel colonies within the amphibole+spinel layer are inconsistent

with simultaneous diffusion-controlled growth of orthopyroxene + spinel and amphibole + spinel layers. This microstructure is difficult to explain except by simultaneous growth of both symplectites. Symplectic aggregates of orthopyroxene + spinel, similar to the plumose colonies in the Risør coronas (fig. 7), separate late intercumulus olivine and plagioclase in oxide-rich gabbros near the contact of the Lower and Middle Zones of the Skaergaard intrusion, East Greenland (Wager and Brown, 1967, fig. 42), where they are obviously magmatic in origin.

8. The presence of texturally and compositionally similar amphibole-spinel symplectite rims on cumulus olivine and ilmenite and on intercumulus amphibole is difficult to reconcile with its being the product of metamorphic reaction between olivine and plagioclase. The assemblage in contact with symplectite at its inner margin may be either orthopyroxene + spinel, ilmenite, spinel, or amphibole. There is no change in microstructure, phase proportion, or composition in symplectite rimming composite ilmenite-spinel grains where it passes along its length from an ilmenite core to a spinel core. Because the microstructures and phase compositions of amphibole-spinel symplectites rimming ilmenite are identical to those on primary and annealed coronas on olivine, but cannot have been formed by solid-state reaction between ilmenite and plagioclase, the metamorphic origin of similar symplectite rims on olivine seems unlikely. Amphibole-spinel symplectite locally separates intercumulus amphibole from plagioclase (figs. 2 and 10) and may do so even where no orthopyroxene or olivine are present (fig. 6, far right).

Interpretation of critical compositional relations in coronas

1. Composition of orthopyroxene is identical in primary and annealed coronas and in the intercumulus magmatic association and is in Fe-Mg exchange equilibrium with olivine.

2. Composition of pargasitic amphibole in primary and annealed coronas on ilmenite is identical to that of amphibole rimming clinopyroxene and occurring as both symplectic and spinel-free grains filling intercumulus spaces in the magmatic association. Pargasitic amphibole in primary and annealed coronas on olivine differs from that in the intercumulus magmatic association only in the slight titanium enrichment of the latter.

3. Compositions of pargasitic amphibole from each of the coronitic and intercumulus magmatic associations in the Risør sample match those of intercumulus pargasitic amphibole in non-

coronitic troctolite from the Kiglapait Intrusion, Labrador (Morse, 1979b) and in corona-free gabbroic rocks from the synorogenic Fongen-Hyllingen layered basic complex, Norway (Wilson *et al.*, 1981) for virtually every cation. Given the close correspondence in composition of coronitic amphibole with those of demonstrated magmatic origin it is very difficult to argue for a metamorphic origin for amphibole in the Risør coronas.

4. Pargasitic amphiboles in the sample from Risør are significantly different in composition from the edenite-tschermakite amphiboles typical of basaltic rocks metamorphosed in the amphibolite facies (Laird and Albee, 1981).

5. The potassium in symplectic amphibole cannot have been derived by the breakdown of olivine and plagioclase. There is no mineralogical source for potassium in this rock.

6. Because both orthopyroxene and amphibole in the coronas are more magnesian than the associated olivine, breakdown of olivine in the core of a corona cannot provide the Mg needed for layer growth unless there is a significant sink for Fe elsewhere in the rock.

7. The problem of Mg-Fe imbalance is compounded for growth of amphibole-spinel symplectite on ilmenite which requires derivation of all Mg in the symplectite from a source outside of the corona. Apart from olivine, there does not appear to be any mineralogical source of Mg. The cusped shape of ilmenite suggests a significant reduction in volume by reaction or resorption. There is no mineralogical sink for the Fe and Ti released on the breakdown of ilmenite. Certainly, the excess Fe and Ti released on growth of ilmenite coronas cannot have been consumed in growth of olivine coronas.

8. Calculated bulk mineralogical compositions of primary and annealed coronas do not match those of product of reaction between olivine and plagioclase.

The compositional problems raised in sections 5 through 8 may be solved by chemical exchange between individual coronas and an external reservoir. This reservoir might be an aqueous fluid (van Lamoen, 1979; Mongkoltip and Ashworth, 1983) or a silicate melt. Chemical exchange and equilibration with a fluid does not provide a satisfactory explanation for the compositional features of amphibole and orthopyroxene listed in sections 1, 2, and 3, however, and does not address the textural problems described in 1 through 8 above. Coupled with the demonstrated instability of the primary corona layer sequence in the model system, the textural and compositional problems enumerated here strongly argue that the metamorphic origin for primary coronas is untenable and that an origin by magmatic processes be examined.

Environment of corona growth

Because diopside + enstatite + spinel are stable at lower temperature and higher pressure than the compositionally equivalent assemblage anorthite + forsterite (Kushiro and Yoder, 1966), it has been suggested that pyroxene-spinel coronas analogous to the amphibole-spinel coronas from Risör form by retrograde reaction on the cooling of gabbro bodies emplaced at high pressures (Griffin and Heier, 1973; Whitney and McLelland, 1973). The common occurrence of cumulus textures in coronitic gabbros is consistent with this mode of origin, whereas it seems unlikely that such textures would survive a prograde metamorphic event.

There are, however, no unequivocal indicators of a high-pressure origin for coronas in the rocks themselves. Because of the segregation of corona minerals into assemblage layers of high variance, and because minerals in the corona are not equilibrated with those in the matrix, the use of element exchange thermobarometers is inappropriate in these rocks. Mongkoltip and Ashworth (1983) summarize geologic evidence that the coronitic gabbros of north-eastern Scotland were emplaced during sillimanite-grade regional metamorphism at pressures of about 5 kbar. There are no other cases in which the timing of gabbro emplacement relative to regional metamorphism is well documented. Droop and Charnley (1985) confirm that pressures in the thermal aureoles of the Newer Gabbros were in the range 4.4–4.7 kbar.

Note that although it is probable that high pressure is a factor in corona development, the coexistence of olivine + plagioclase in Kiglapait troctolite, emplaced at a pressure of 4 kbar (Berg, 1977; Morse, 1979a), and in Fongen-Hyllingen gabbros, emplaced during metamorphism at 5 to 6 kbar (Wilson *et al.*, 1981), again argue that the instability of olivine and plagioclase in contact does not provide the driving force for corona formation.

Liquidus phase relations in the basaltic system at high pressures

Phase relations in a simplified basaltic system that crystallizes amphibole and spinel at high pressure have not been fully determined. However, Presnall *et al.* (1979) have compiled and interpolated liquidus phase relations in the simplified basalt tetrahedron forsterite-diopside-anorthite-silica, based on the bounding planes forsterite-diopside-anorthite (Presnall *et al.*, 1978) and forsterite-diopside-silica (Kushiro, 1969). This system provides a useful model for the earlier stages in the magmatic evolution of the coronitic gabbro from Risör.

The principal change in the bounding ternary

systems at high pressure is the disappearance of the forsterite-anorthite cotectic and its replacement by a diopside-spinel cotectic at 5 kbar in forsterite-diopside-anorthite (Presnall *et al.*, 1978, fig. 5; Morse, 1980, fig. 18.11) and by an enstatite-spinel cotectic at a pressure less than 7 kbar in forsterite-anorthite-silica (Morse, 1980, fig. 18.17). Thus a liquid crystallizing olivine that would have been driven on to the forsterite-anorthite cotectic at low pressure to form a troctolite, evolves to an olivine-free gabbro along the diopside-enstatite-anorthite cotectic curve. Along this path, diopside and/or enstatite crystallize in a cotectic relation with spinel prior to its elimination at the diopside-enstatite-anorthite-spinel peritectic. The coexistence of forsterite and anorthite is thus precluded at pressures greater than 5 kbar. The binary forsterite-enstatite peritectic persists to at least 7 kbar in the dry system (Presnall *et al.*, 1979) and to 20 kbar in the presence of water (Kushiro *et al.*, 1968).

Limited experimental data in the system forsterite-plagioclase (AN₅₀)-silica-H₂O at 15 kbar (Kushiro, 1974) show that the cotectic assemblage pargasite-forsterite evolves to pargasite-enstatite by elimination of forsterite by peritectic reaction and thence to pargasite-plagioclase. Forsterite and plagioclase do not coexist and the binary forsterite-enstatite peritectic relation is retained. The status of spinel in this system is uncertain as phase relations were determined for a limited range of compositions.

Normative composition of coronitic and non-coronitic troctolites

The normative compositions of twenty-five coronitic gabbros and troctolites from the Risör-Söndeled district (Starmer, 1969) plot within the spinel volume in the system forsterite-diopside-anorthite-silica at 7 to 10 kbar (Presnall *et al.*, 1979; Morse, 1980) and cross into the anorthite field. Although the bulk composition of the Kiglapait intrusion, which is not coronitic, plots within this volume (Morse, 1981) as does the chilled margin of the nearby Hettash troctolite (Berg, 1980), the compositions of Kiglapait border zone rocks, representing crystallization of less than 5% of the volume of the intrusion, lie far outside of this volume. Compositions of troctolites from the Kiglapait and Hettash intrusions scatter widely and do not lie along the plagioclase-olivine cotectic (Morse, 1979b, 1981; Berg, 1980), while those of the Risör rocks form a tight cluster within the spinel volume. The normative compositions of rocks from feeders to the synorogenic but non-coronitic Fongen-Hyllingen complex, Norway, plot outside the spinel field (Wilson *et al.*, 1981).

Intercumulus magmatic association

The rimming of olivine by orthopyroxene and the filling in of triangular spaces between plagioclase laths by clinopyroxene rimmed by amphibole are readily interpreted in terms of magmatic processes. Olivine, spinel, ilmenite, and plagioclase are interpreted as cumulus phases. The orthopyroxene rim on olivine is the result of peritectic reaction of olivine with intercumulus liquid. Adcumulus growth of plagioclase and orthopyroxene from the trapped intercumulus liquid drives the liquid composition into the clinopyroxene volume and ultimately into an amphibole field. The amphibole-spinel symplectite on ilmenite and on olivine rimmed by orthopyroxene and clinopyroxene may represent residual liquid crystallized at a eutectic.

Spinel crystallizes from liquids with compositions within the spinel field of the simplified basalt tetrahedron, or along its surface. Liquid compositions can leave the surface of this volume only by resorption of all spinel previously crystallized. Segregation of forsterite from a liquid on the spinel surface will drive the liquid composition into the anorthite or diopside field, while segregation of anorthite will drive the liquid into the forsterite or enstatite field. Thus the development of orthopyroxene and clinopyroxene in the intercumulus association is exactly as expected as a result of fractionation of cumulus olivine and plagioclase.

Primary coronas

The sequence of events in the evolution of the primary coronas on olivine by magmatic processes is envisioned as follows. Cumulus olivine reacts with liquid to produce orthopyroxene. Continued reaction drives the liquid on to the orthopyroxene-spinel cotectic surface and the orthopyroxene-spinel symplectite layer is formed. The layer breaks down at the equivalent of the diopside-enstatite-anorthite-spinel peritectic in the system capable of crystallizing amphibole. Amphibole-spinel symplectite crystallized either along a cotectic or at an eutectic with plagioclase. Crystallization of amphibole-spinel symplectite in the vicinity of ilmenite grains begins when the liquid becomes saturated in amphibole.

The timing of events in the crystallization of primary coronas from the main batch of melt, relative to events in the crystallization of trapped intercumulus liquid is recorded where mineral assemblage layers of the primary corona and the magmatic association are in contact along the rim of a single olivine crystal. The contact between intercumulus orthopyroxene and clinopyroxene appears to lie at the same horizon as the contact

between orthopyroxene and orthopyroxene-spinel symplectite in the corona. Thus crystallization of clinopyroxene in the magmatic association coincided with crystallization of the main batch of melt along the orthopyroxene-spinel cotectic surface. The beginning of crystallization of amphibole in the magmatic assemblage and of amphibole-spinel symplectite in the coronas coincided in time.

The common occurrence of columnar impingement orthopyroxene separating grains of cumulus olivine and the single instance in which orthopyroxene, rimming olivine, is in contact with cumulus plagioclase, indicate that grains of cumulus olivine were rimmed by orthopyroxene before coming into contact with laths of cumulus plagioclase. The amphibole-spinel symplectite may have developed in an intercumulus environment in which trapped liquid separated olivine rimmed successively by orthopyroxene and orthopyroxene-spinel symplectite and cumulus plagioclase. The apparent cross-cutting of plagioclase by coronas on olivine may result from accumulus growth of plagioclase around the corona and does not necessarily imply consumption of plagioclase by reaction. Similar textural relations between plagioclase and olivine occur in troctolites in which no coronas occur (Morse, 1979b).

There is one isolated case in which juxtaposed coronitic and postcumulus magmatic microstructures can be shown to have developed prior to having come into contact, and which shows that primary corona growth and annealing were sequential rather than contemporaneous processes. Amphibole-spinel symplectite of the primary corona is in contact with the outer margin of magmatic amphibole-spinel symplectite on a grain of postcumulus magmatic amphibole (fig. 6, right centre). As there is now no plagioclase in contact with coronitic symplectite, this relation suggests that the primary corona microstructure evolved in contact with magma before the cumulus olivine with its coronitic layers came into contact with magmatic amphibole. That part of the coronitic amphibole-spinel symplectite that is annealed has the same optical orientation as the adjacent magmatic amphibole. Thus, annealing took place *in situ* after the corona came into contact with magmatic amphibole.

Morse (1979a) suggested a mechanism by which olivine and plagioclase nucleate and grow at the roof and floor, respectively, of a magma body from which layered troctolites accumulated. Thus olivine with its orthopyroxene and orthopyroxene-spinel rims may have grown prior to accumulation with plagioclase on the floor of the intrusion.

The reason that coronas formed in the troctolitic

rocks from Risör, which may have crystallized during amphibolite-facies metamorphism, while they did not form at Kiglapait where intrusion depth corresponded to pressure of 4 kbar (Berg, 1977; Morse, 1979a) or in the Fongen-Hyllingen complex, synorogenically emplaced at pressures of 5 to 6 kbar (Wilson *et al.*, 1981), appears to lie in the preservation of the orthopyroxene/olivine rimming relation in the rocks at Risör. The critical step in the formation of coronas may be the requirement that the composition of the liquid reach the orthopyroxene-spinel cotectic surface and that two-phase assemblage crystallize as a rim on orthopyroxene. The emplacement pressure at Kiglapait was probably below that of the enstatite-spinel cotectic, and thus too low for corona formation while the bulk composition of the Fongen-Hyllingen magmas lay outside of the critical spinel compositional field.

Annealed coronas

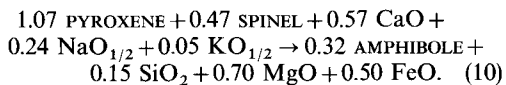
Symplectite of the primary coronas consists of fan-shaped grains of pargasite that open toward plagioclase and are ribbed by rods of spinel. On annealing to a single grain, low-angle grain boundaries disappear and spinel rods rotate into parallel. Primary orthopyroxene, initially radial to layer contacts, anneals to a single grain, rimming olivine. Irregular discontinuous layers and plumes of orthopyroxene-spinel symplectite disappear on annealing and a monomineralic layer of pargasite forms between orthopyroxene and the annealed amphibole symplectite. Note, however, that because orthopyroxene may retain its primary microstructure even when amphibole is fully annealed (fig. 10), the microstructure of the amphibole symplectite transforms more readily than does that of the orthopyroxene layer.

The transition between a corona with the primary microstructure and its annealed counterpart occurs abruptly along the length of the layer (fig. 12A and B, fig. 4, lower right). The transition commonly occurs at a corner on the olivine core, where the layers bend sharply. If the annealing processes involve rotation of the structure of amphibole and orthopyroxene grains into parallel with the template provided by its magmatic counterpart, the propagation of the anneal along the layer may be impeded by a sharp change in orientation as at a corner.

Details of the annealing process can be seen in the progressive changes in microstructure within a few hundred microns of the contact with the layers of the primary corona (fig. 12B). The contact between amphibole and orthopyroxene in the annealed microstructure lies at the same position

as the contact between orthopyroxene-spinel symplectite and orthopyroxene in the primary microstructure. Thus, both amphibole-spinel symplectite and amphibole occupy the former position of the orthopyroxene-spinel symplectite. At this point the amphibole layer is only about 3 μm wide. About 70 μm from the primary/annealed junction along strike of the layers, the monomineralic amphibole layer abruptly widens to about 15 μm . The amphibole:orthopyroxene layer contact moved into orthopyroxene, while the contact between amphibole and amphibole-spinel symplectite shows very little displacement. Note that the concentration of spinel in the inner part of the symplectite layer is reduced and that a spinel-free band developed a few microns into the symplectite layer. Further away from the contact with primary symplectite, the monomineralic amphibole layer widens, the orthopyroxene layer thins, and symplectitic spinel in the inner part of the layer becomes more rod-like (fig. 9B). These observations suggest that the monomineralic amphibole layer grows at the contact with symplectite by dissolution of spinel and that it also grows at the expense of orthopyroxene.

Breakdown of the orthopyroxene-spinel symplectite and formation of a monomineralic amphibole layer requires significant changes in local bulk composition. Because the monomineralic amphibole layer has not been observed in contact with orthopyroxene-spinel symplectite, it is likely that the initial breakdown reaction involves formation of an amphibole-spinel assemblage until all spinel in the orthopyroxene-spinel layer is consumed. Calculation of the net reaction using equation (1) requires an arbitrary choice of reference frame. Because any CaO , $\text{NaO}_{1/2}$, $\text{KO}_{1/2}$ or $\text{AlO}_{3/2}$ released in the reaction must either diffuse into the olivine core or diffuse up-gradient to plagioclase, the volume factor must be such that these four components are either consumed or held fixed on reaction. The net reaction for growth of amphibole-spinel symplectite at the expense of orthopyroxene-spinel symplectite for the limiting volume factor of 1.02, corresponding to an $\text{AlO}_{3/2}$ -fixed frame, is



Thus, the early stages of the annealing process necessarily involve consumption of both olivine and plagioclase. Reaction (10) should continue until all orthopyroxene-spinel symplectite is consumed, at which point the exchange cycle described by reactions (5)–(8) should be established.

ORIGIN OF CORONAS

The two features of coronitic gabbros that, from the earliest studies, have strongly argued for a metamorphic origin for coronas are the consistent occurrence of orthopyroxene and symplectite layers separating olivine and plagioclase and the restricted occurrence of coronitic gabbros to amphibolite-facies and granulite-facies metamorphic terranes. However, the textural and compositional features described above show that while primary coronas from Risör cannot have been formed by reaction between olivine and plagioclase, these features are consistent with crystallization from a spinel-saturated basaltic magma at high pressure. It is concluded that magmas that crystallize troctolite on the plagioclase-olivine cotectic at pressures below about 5 kbar, form coronites at pressures greater than 5 kbar. Textural evidence has been presented showing that the annealed microstructure evolved sequentially from that of the primary coronas. Irreversible thermodynamic calculations show that the mineral assemblage layer sequence of primary coronas in the model system is diffusionally unstable and that this instability may provide the driving force for their spontaneous transformation to the stable mineral assemblage layer sequence of the annealed coronas.

The conclusion of this study that the primary growth of orthopyroxene:amphibole + spinel coronas is a magmatic phenomenon is of widespread applicability. Although the coronas described by Mason (1967) from the Sulitjelma gabbro, Norway and by Mongkoltip and Ashworth (1983) from the Huntly gabbro, Scotland, have the annealed microstructure, the writer has observed both the primary and annealed microstructures in coronitic troctolites from these localities. The bulk composition of coronitic gabbro from Sulitjelma (sample S96, Mason, 1967, 1971) lies within the spinel volume of the basalt tetrahedron, as required by this model. The microstructural features of olivine coronas in gabbros from Susimäki and Riuttamaa, Finland, described in detail by van Lamoen (1979) are identical to those of the primary coronas described here. It is thus reasonable to conclude that the coronas of orthopyroxene and pargasitic amphibole + spinel symplectite that occur quite widely in troctolitic gabbros are magmatic in origin.

Primary orthopyroxene:amphibole + spinel coronas from Risör form by normal processes of magmatic crystallization of a troctolitic magma at high pressure and are subsequently modified by solid-state processes of annealing and elemental redistribution. Garnet-bearing coronas in meta-troctolite from granulite-facies terranes commonly

preserve a clinopyroxene-spinel symplectite that is interpreted as having developed prior to the garnet-producing reaction (Griffen and Heier, 1973; Whitney and McLelland, 1973; McLelland and Whitney, 1980a). It is suggested here that the columnar impingement orthopyroxene layer (Griffen and Heier, 1973) and the clinopyroxene-spinel symplectite are the products of magmatic processes similar to those that produced the primary corona microstructure at Risör, but which operated at pressures greater than about 9 kbar (Presnall *et al.*, 1979, fig. 3).

Acknowledgements. I am grateful to Ben Harte and the Metamorphic Studies Group of the Mineralogical Society for providing the opportunity to present this work at the Mechanisms of Reaction Symposium. Kate Brodie and Ernie Rutter were gracious and hard-working hosts for the associated workshop at Imperial College. Stuart Agrell and Graham Chinner made my sabbatical leave at Cambridge, during which this study was begun, an enjoyable one. I thank John Ashworth for a thorough review and valiant attempt to separate the author from his magmatic model. Work on coronas was supported by NSF grant EAR-80-25373.

REFERENCES

- Berg, J. H. (1977) Regional geobarometry in the contact aureoles of the anorthositic Nain complex, Labrador. *J. Petrol.* **18**, 399-430.
- (1980) Snowflake troctolite in the Hettash intrusion: evidence for magma mixing and supercooling in a plutonic environment. *Contrib. Mineral. Petrol.* **72**, 339-51.
- Brögger, W. C. (1934) On several Archaean rocks from the south coast of Norway II. The south Norwegian hyperites and their metamorphism. *Skrifter utgitt av Det Norske Videnskaps-Akademi i Oslo*, I. Matem.-Naturvid Klasse, 421 pp.
- Droop, G. T. P., and Charnley, N. R. (1985) Comparative geobarometry of pelitic hornfelses associated with the Newer Gabbros: a preliminary study. *J. Geol. Soc. London*, **142**, 53-62.
- Fisher, G. W. (1973) Nonequilibrium thermodynamics as a model for diffusion-controlled metamorphic processes. *Am. J. Sci.* **273**, 897-924.
- (1977) Nonequilibrium thermodynamics in metamorphism. In *Thermodynamics in Geology* (D. Fraser, ed.), D. Reidel, Dordrecht, pp. 381-403.
- Frantz, J. D., and Mao, H. K. (1975) Bimetasomatism resulting from intergranular diffusion: multiminerale zone sequences. *Carnegie Inst. Wash. Yearb.* **74**, 417-24.
- Gresens, R. L. (1967) Composition-volume relationships of metasomatism. *Chem. Geol.* **2**, 47-65.
- Grieve, R. A. F., and Gittins, J. (1975) Composition and formation of coronas in the Haddlington gabbro, Ontario, Canada. *Can. J. Earth Sci.* **12**, 289-99.
- Griffin, W. L., and Heier, K. S. (1973) Petrological implications of some corona structures. *Lithos*, **6**, 315-35.

- Harker, A. (1909) *The Natural History of Igneous Rocks*. Hafner, New York, 384 pp.
- Joesten, R. (1977) Evolution of mineral assemblage zoning in diffusion metasomatism. *Geochim. Cosmochim. Acta*, **41**, 649-70.
- (1978) Diffusion-controlled growth of pyroxene-spinel coronas between forsterite and anorthite in the system CaO-MgO-Al₂O₃-SiO₂. *Geol. Soc. Am. Abstr. Program*, **10**, 429.
- Kuo, L.-C., and Kirkpatrick, R. J. (1985) Kinetics of crystal dissolution in the system diopside-forsterite-silica. *Am. J. Sci.* **285**, 51-90.
- Kushiro, I. (1969) The system forsterite-diopside-silica with and without water at high pressures. *Am. J. Sci.* **267-A**, 269-94.
- (1974) Melting of hydrous upper mantle and possible generation of andesitic magma: an approach from synthetic systems. *Earth Planet. Sci. Lett.* **22**, 294-9.
- and Yoder, H. S., Jr. (1966) Anorthite-forsterite and anorthite-enstatite reactions and their bearing on the basalt-eclogite transformation. *J. Petrol.* **5**, 195-218.
- and Nishikawa, M. (1968) Effect of water on the melting of enstatite. *Geol. Soc. Am. Bull.* **79**, 1685-92.
- Laird, J., and Albee, A. L. (1981) Pressure, temperature and time indicators in mafic schist: their application to reconstructing the polymetamorphic history of Vermont. *Am. J. Sci.* **281**, 127-75.
- McLelland, J. M., and Whitney, P. R. (1977) The origin of garnet in the anorthosite-charnockite suite of the Adirondacks. *Contrib. Mineral. Petrol.* **60**, 161-81.
- (1980a) A generalized garnet-forming reaction for meta-igneous rocks in the Adirondacks. *Ibid.* **72**, 111-22.
- (1980b) Compositional controls on spinel clouding and garnet formation in plagioclase of olivine metagabbros, Adirondack Mountains, New York. *Ibid.* **73**, 243-51.
- Mason, R. (1967) Electron-probe microanalysis of coronas in a troctolite from Sulitjelma, Norway. *Mineral. Mag.* **36**, 504-14.
- (1971) The chemistry and structure of the Sulitjelma gabbro. *Nor. Geol. Unders.* **269**, 108-42.
- Medaris, L. G. (1969) Partitioning of Fe²⁺ and Mg²⁺ between coexisting synthetic olivine and orthopyroxene. *Am. J. Sci.* **267**, 945-68.
- Mongkoltip, P., and Ashworth, J. R. (1983) Quantitative estimation of and open-system symplectite-forming reaction: restricted diffusion of Al and Si in coronas around olivine. *J. Petrol.* **24**, 635-61.
- Morse, S. A. (1979a) Kiglapait geochemistry I: Systematics, sampling, and density. *Ibid.* **20**, 555-90.
- (1979b) Kiglapait geochemistry II: Petrography. *Ibid.* **20**, 591-624.
- (1980) *Basalts and Phase Diagrams*. Springer-Verlag, New York, 493 pp.
- (1981) Kiglapait geochemistry IV: The major elements. *Geochim. Cosmochim. Acta*, **45**, 461-79.
- Murthy, M. V. N. (1958) Coronites from India and their bearing on the origin of coronas. *Geol. Soc. Am. Bull.* **68**, 23-38.
- Nishiyama, T. (1983) Steady diffusion model for olivine-plagioclase corona growth. *Geochim. Cosmochim. Acta*, **47**, 283-94.
- Nockolds, S. R., Knox, R. W. O'B., and Chinner, G. A. (1978) *Petrology for Students*. Cambridge University Press, Cambridge, 435 pp.
- Presnall, D. C., Dixon, S. A., Dixon, J. R., O'Donnell, T. H., Schrock, R. L., and Dycus, D. W. (1978) Liquidus phase relations on the join diopside-forsterite-anorthite from 1 atm to 20 kbar: their bearing on the generation and crystallization of basaltic magma. *Contrib. Mineral. Petrol.* **66**, 203-20.
- Dixon, J. R., O'Donnell, T. H., and Dixon, S. A. (1979) Generation of mid-ocean ridge tholeiites. *J. Petrol.* **20**, 3-36.
- Reynolds, R. C., Jr., and Frederickson, A. F. (1962) Corona development in Norwegian hyperites and its bearing on the metamorphic facies concept. *Geol. Soc. Am. Bull.* **73**, 59-72.
- Sederholm, J. (1916) On synantectic minerals and related phenomena. *Comm. Geol. Finlande Bull.* **48**, 1-148.
- Starmer, I. C. (1969) Basic plutonic intrusions of the Risør-Söndeled area, south Norway: the original lithologies and their metamorphism. *Norsk Geol. Tidssk.* **49**, 403-31.
- Statham, P. J. (1976) A comparative study of techniques for quantitative analysis of the X-ray spectra obtained with a Si(Li) detector. *X-ray Spectrom.* **5**, 16-28.
- Sweatman, T. R., and Long, J. V. P. (1969) Quantitative electron-probe microanalysis of rock forming minerals. *J. Petrol.* **16**, 332-79.
- Törnebohm, A. E. (1877) Om Sveriges viktigare Diabas- och Gabbro-Arter. *Kgl. Sveska Vetenskaps-Akademiens Handlingar*, B.14, No. 13.
- van Lamoen, H. (1979) Coronas in olivine gabbros and iron ores from Susimäke and Riuttamaa, Finland. *Contrib. Mineral. Petrol.* **68**, 259-68.
- Wager, L. R., and Brown, G. M. (1967) *Layered Igneous Rocks*. W. H. Freeman and Co., San Francisco, 588 pp.
- Whitney, P. R., and McLelland, J. M. (1973) Origin of coronas in metagabbros of the Adirondack Mts, N.Y. *Contrib. Mineral. Petrol.* **39**, 81-98.
- Wilson, R., Esbensen, K. H., and Thy, P. (1981) Igneous petrology of the synorogenic Fongen-Hyllingen layered basic complex, south-central Scandinavian Caledonides. *J. Petrol.* **22**, 584-627.

[Revised manuscript received 5 February 1986]